The Meteoritical Society

Meteoritics & Planetary Science 57, Nr 12, 2170–2191 (2022)
doi: 10.1111/maps.13922

Terrestrial ages of seven meteorite strewn fields and two single unpaired meteorites from the Sultanate of Oman determined using ^{14}C and ^{10}Be

Malgorzata U. SLIZ[1,2], Beda A. HOFMANN[2,3]*, Ingo LEYA[1], Sönke SZIDAT[4], Christophe ESPIC[5], Jérôme GATTACCECA[5], Régis BRAUCHER[5], Daniel BORSCHNECK[5], Edwin GNOS[6], and ASTER Team[5†]

[1]Space Research and Planetary Sciences, University of Bern, Sidlerstrasse 5, 3012 Bern, Switzerland
[2]Natural History Museum Bern, Bernastrasse 15, 3005 Bern, Switzerland
[3]Institute of Geological Sciences, University of Bern, Baltzerstrasse 1+3, 3005 Bern, Switzerland
[4]Department of Chemistry and Biochemistry & Oeschger Center for Climate Change Research, University of Bern, Freiestrasse 3, 3012 Bern, Switzerland
[5]CNRS, Aix Marseille Univ, IRD, INRAE, CEREGE, Aix-en-Provence, France
[6]Natural History Museum of Geneva, Route de Malagnou 1, 1208 Geneva, Switzerland
*Corresponding author. E-mail: beda.hofmann@geo.unibe.ch

(Received 01 July 2022; revision accepted 17 October 2022)

Abstract–Through the investigation of terrestrial ages of meteorites from Oman, we aim to better understand the time scales of meteorite accumulation and erosion in Oman and the meteorite flux in the past. Here, we present ^{14}C and ^{14}C-^{10}Be terrestrial ages of seven ordinary chondrite strewn fields and two unpaired single meteorites from the Sultanate of Oman. After critical evaluation of multiple data for each strewn field, we propose "best estimate terrestrial ages," typically based on $^{14}C/^{10}Be$. For objects for which complex irradiation histories are known or suspected, terrestrial ages were calculated solely using ^{14}C. The best estimate strewn field ages range from 8.1 ± 3.0 ka (SaU 001) to 35.2 ± 5.1 ka (Dho 005). Including two previously dated strewn fields, the mean and median age of nine Oman strewn fields is 15.9 ± 12.3 and 13.6 ka, respectively. The new data show a general good agreement with data previously obtained in a different laboratory, and we observe a similar general correlation between strewn field ages and mean weathering grade as in previous work based on individual meteorites. Weathering degree W4 is reached for dated samples after 20–35 ka. While the age statistics of strewn fields does not show the previously observed lack of young events, the low abundance of young (0–5 ka) individual meteorites as compared with older (~20 ka) meteorites is confirmed by our data and remains unexplained.

INTRODUCTION

Studies of meteorites shed light on the history of the solar system, helping us to understand its chemical and physical evolution through time. Fragments of asteroids and pieces from Mars and the Moon arrive on the Earth's surface as meteorites. While some of them can be observed falling, most of them are collected years after their fall during field campaigns to hot and cold deserts, where their recovery is easier than in forested or densely populated areas. The accumulation and erosion of meteorites depends on the environmental conditions (e.g., Jull, 2006). The conditions prevailing in hot and cold deserts, that is, lack of free-running water, enable meteorites to survive for thousands (most hot deserts; Al-Kathiri et al., 2005; Bevan, 2006; Jull, 2006; Jull et al., 1993; Jull, Cielaszyk et al., 1998; Kring et al., 2001) or even millions of years (some hot deserts, cold deserts; Cassidy, 2003; Gattacceca et al., 2011; Jull, 2006). The conditions supporting or limiting meteorite preservation differ from one desert to another—meteorites in the deserts of the Sultanate of

[†]ASTER Team: G. Aumaître, D. Bourlès, K. Keddadouche.

Oman, North Africa, United States, and Australia survive 30–50 ka on average, whereas samples found in the Atacama Desert and in Antarctica can have terrestrial ages of as high as 2 Ma (Drouard et al., 2019; Jull, 2006).

Of the 69,838 approved meteorites listed in the Meteoritical Bulletin Database (as of July 1, 2022), 62.1% are finds from Antarctica. The vast majority of the rest are hot desert finds: 19.9% are from North Africa, 6.0% from Arabia, 3.3% from Chile, and 0.5% from Iran. This demonstrates the importance of hot desert finds as a source of meteorites. Numerous studies have investigated aspects of hot desert meteorites with a focus on terrestrial ages and weathering. Detailed studies were performed in the following areas: Northern Africa (Aboulahris et al., 2019; Bischoff & Geiger, 1995; Laridhi Ouazaa et al., 2009; Schlüter et al., 2002), the western United States (Jull et al., 1993; Zolensky et al., 1990), the Nullarbor Plain of Australia (Bevan et al., 1998; Jull et al., 2010), the Atacama Desert (Gattacceca et al., 2011; Hutzler et al., 2016; Munayco et al., 2013; Muñoz et al., 2007), Iran (Pourkhorsandi et al., 2019), and the Arabian Peninsula, most notably Oman (Al-Kathiri et al., 2005; Zurfluh et al., 2016), Saudi Arabia (Hofmann et al., 2018), and the United Arab Emirates (Hezel et al., 2011).

Currently, many of the meteorites found in the Sultanate of Oman are studied by our group (Mészáros et al., 2018; Sliz et al., 2018, 2019, 2020), particularly with respect to the terrestrial ages, by using the cosmogenic radionuclide ^{14}C. Note that the systematic investigation of terrestrial ages of meteorites is crucial for studying the time scale of meteorite accumulation (Jull, 2006), effects of erosion on the meteorite population on Earth (Al-Kathiri et al., 2005; Hutzler et al., 2016; Jull et al., 1993; Pourkhorsandi et al., 2019; Zurfluh et al., 2016), and most importantly for studying the meteorite flux over time (Bland et al., 1996; Halliday et al., 1989). The ^{14}C terrestrial age dating is a well-established technique with an immense potential but is currently applied to meteorites only in very few laboratories worldwide (Jull et al., 2013; Mészáros et al., 2018; Minami & Nakamura, 2001; Minami et al., 2006; Sliz et al., 2020).

The cosmogenic radionuclide ^{14}C is produced in meteorites by spallation reactions induced by primary and secondary galactic cosmic ray particles (Reedy & Arnold, 1972). The major target element for cosmogenic ^{14}C production in stony meteorites and planetary surfaces is oxygen (O), though spallation reactions on Mg, Al, Si, Ca, Fe, and Ni also produce in situ ^{14}C; however, their contributions are significantly smaller (Born & Begemann, 1975; Leya et al., 2001). Aside from production in space, cosmogenic in situ ^{14}C is also produced while the meteorite is on the Earth's surface, that is, through terrestrial cosmogenic nuclide production. However, contributions from terrestrial production are considered negligible as they are two to three orders of magnitude smaller than the production rates in space (Jull et al., 2013; Lifton et al., 2001). In addition, processes on Earth such as weathering and possibly biological processes may add ^{14}C to the meteorite, affecting its ^{14}C budget (Jull, Courtney et al., 1998; Lee et al., 2017; Zurfluh et al., 2016). Carbon-14 has a half-life of 5700 ± 30 yr (National Nuclear Center, Brookhaven National Laboratory) and is the rarest naturally occurring isotope of carbon with a $^{14}C/^{12}C$ ratio of 1.1694×10^{-12} in modern terrestrial carbon (National Nuclear Center, Brookhaven National Laboratory). The bulk ^{14}C activity concentrations of recently fallen ordinary chondrites range from 35 to 59 dpm kg^{-1} (Jull et al., 1989). Assuming a carbon content for ordinary chondrites of about 0.2 wt% (Makjanic et al., 1993), we calculate $^{14}C/^{12}C$ ratios in freshly fallen ordinary chondrite samples in the range of $1.51–2.54 \times 10^{-12}$. Based on the fact that this ratio is similar or even slightly higher than the atmospheric value, terrestrial contamination can, in principle, compromise studies of meteorites with long terrestrial ages.

In addition to the problem of contamination, there is another difficulty when using ^{14}C activity concentrations for terrestrial age determinations. The ^{14}C concentrations in meteorites are known to vary significantly with pre-atmospheric size of the meteorite and depth of the sample below the pre-atmospheric surface; size and depth are usually considered together as the "shielding depth." A method that internally corrects for the shielding dependence uses $^{14}C/^{10}Be$ activity concentration ratios instead of relying on ^{14}C activity concentrations only. The so-called ^{14}C-^{10}Be terrestrial ages are less dependent on shielding and are therefore more reliable than ages determined using ^{14}C only (Jull, 2006). Beryllium-10 is a long-lived radionuclide with a half-life of $1.387 \pm 0.012 \times 10^6$ yr (Korschinek et al., 2010) that is predominantly produced by spallation reactions on O (e.g., David & Leya, 2019), that is, from the same target element as ^{14}C. Specific activity concentrations in bulk H, L, and LL ordinary chondrites are in the range of 20 and 22 dpm kg^{-1}, respectively (Nishiizumi, 1995; Nishiizumi et al., 1989). The very similar reaction pathways and the fact that both radionuclides are produced from the same target elements make the $^{14}C/^{10}Be$ production rate ratio almost independent of shielding (Jull, 2006). The $^{14}C/^{10}Be$ production rate ratio is currently assumed to be 2.5 ± 0.2, based on data from recently fallen

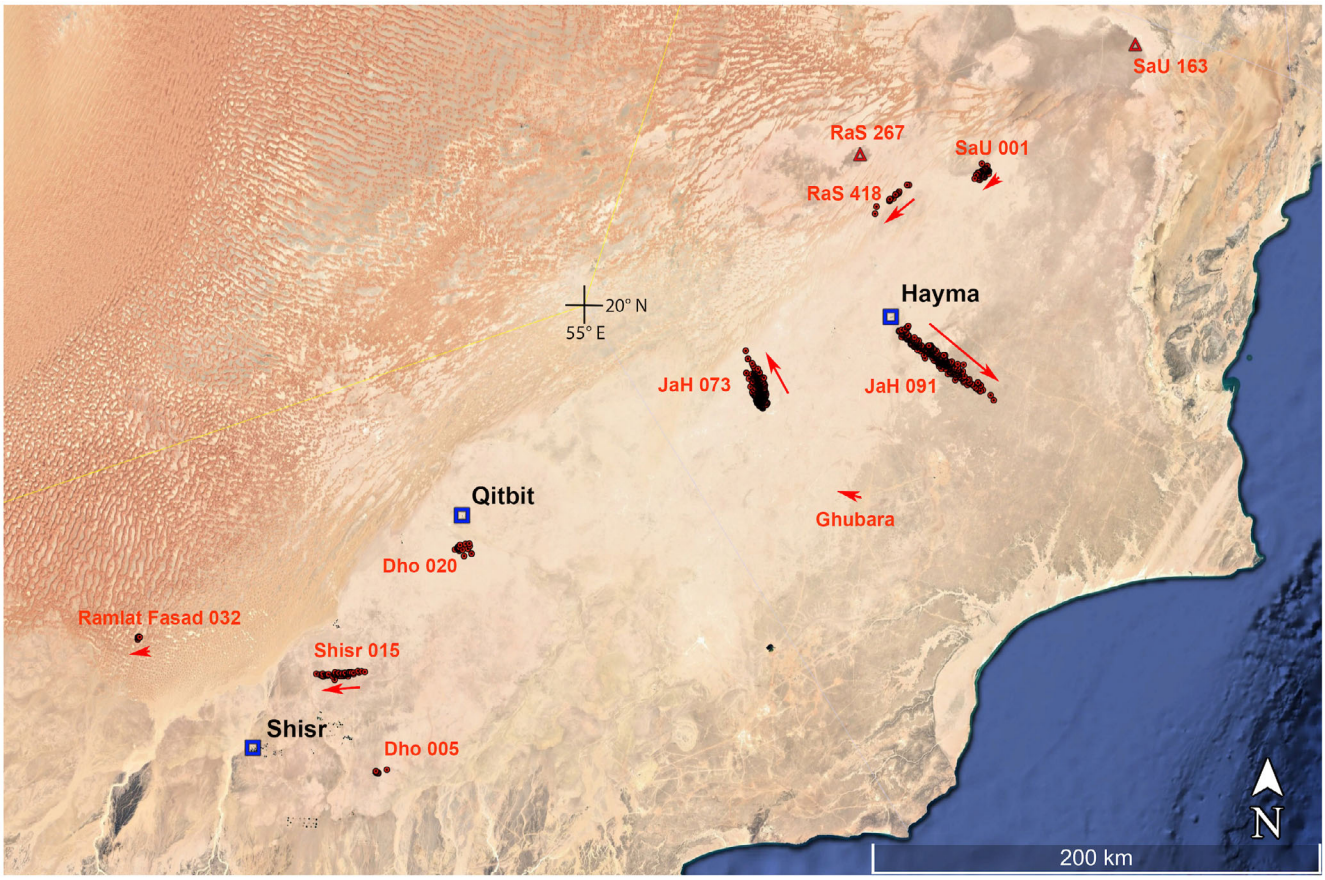

Fig. 1. Location of the studied strewn fields and individual samples (triangles) in south central Oman with indication of the direction of fall (where known). Also shown are the locations of the strewn fields Ghubara and Ramlat Fasad 032, mentioned in the text. See Fig. S1 for individual strewn fields. Note the predominance of sand-free areas in the southeastern parts and sand-dominated areas of the Rub'al-Khali in the northwest. Image: Google Earth.

meteorites (Jull et al., 2001; Kring et al., 2001; Welten et al., 2001). Note, however, that the ^{14}C-^{10}Be method can only be used if ^{10}Be is in saturation, that is, if the meteorite's exposure in space (cosmic ray exposure age) is longer than approximately 7–8 Ma (Jull et al., 2013). In contrast to ^{10}Be, ^{14}C reaches saturation within only approximately 50 ka of exposure, assuming no losses of the radionuclide due to diffusion and/or recoil.

In this study, we focus on determining ^{14}C-^{10}Be terrestrial ages of meteorite strewn fields found in the Sultanate of Oman. A strewn field refers to meteorites of a single fall, dispersed over an area as a result of its fragmentation in the Earth's atmosphere. Our work focuses on meteorite strewn fields because of their distinct features, that is, the high density of meteorites, the size sorting of fragments, and the known orientation of the fall. Most importantly, all meteorites belonging to the same strewn field must have an identical terrestrial age. Note that compared to other falls, meteorite strewn fields are derived from relatively large meteoroids for which shielding effects, which we try to eliminate or at least to reduce by using ^{14}C-^{10}Be terrestrial age dating, are likely relevant.

Oman has very favorable conditions for the preservation and search for meteorites due to its very extensive light-colored and geologically stable sand-poor plains of ~97,000 km^2 forming a 150–200 km wide belt between the Arabian sea and the lower lying Rub'al-Khali sand desert (~42,000 km^2 in Oman, Fig. 1). The plateau areas with few wadis are at an altitude of 100–400 m and consist of essentially flat-lying limestones of Miocene, Oligocene, and Eocene age. Locally horizontal bedding is disturbed as a result of salt tectonics with several diapirs reaching the surface (Le Métour et al., 1993). The peneplain is typically covered by a regolithic soil containing bedrock fragments, wind-blown material, and in places by calcrete or gypcrete. Toward the interior of the Arabian mainland, plains are partially to entirely covered by sand dunes, constituting the vast Rub'al-Khali desert at plain altitudes of 60–300 m in Oman. A system of alluvial fans forms a

transitional belt to the Oman Mountains in the north and to the Dhofar Mountains in the south. Detailed descriptions of the geological features relevant for meteorite accumulations are given by Al-Kathiri et al. (2005), Fookes and Lee (2009), Hofmann et al. (2018), and Rosén et al. (2021). The climate of south central Oman is arid with an annual precipitation of <25 to 50 mm (Edgell, 2006), the mean annual temperature in Hayma (19°57.5′N 56°16.5′E) is 28.6 °C (average-weather.com). Despite the aridity, humidity is brought into the desert by fog leading to common wetting of rock surfaces in mornings during winter months. This is expressed by an abundance of lichen on rocks in near-coastal areas (Lee et al., 2017).

The Omani-Swiss meteorite search (OSMS) program started in 2001 (Al-Kathiri et al., 2005; Gnos et al., 2009; Hofmann, 2010; Hofmann et al., 2003, 2011, 2014). Since then, yearly search campaigns (19 in total until 2020) resulted in a large collection of meteorites, all well documented in terms of find locations, pairing corrections, and classification. In the last 19 yr, large parts of the desert areas in Oman have already been searched, yet every next campaign brings new interesting meteorite finds. Since 2014–2015, the major focus of the campaigns has been on the dune-rich areas in the southwest of Oman, where sediment age data indicate surface ages that range from <1 ka to approximately 100 ka (Matter et al., 2015). Current and future research are focused on the so-called "meteorite-rich" areas, that is, areas with a high density of meteorites. In recent fieldwork, strongly deflated small areas close to large star dunes, the so-called blowouts, were also a major target of the search campaigns. The find density in these areas is approximately 30 meteorites per km^2, that is, well above the previously determined average density of 1–2 finds per km^2 typical for Oman (data used from 2001 to 2014 search period; OSMS database; Hofmann et al., 2014, 2018; Rosén et al., 2021).

The ^{14}C extraction line at the University of Bern (Mészáros et al., 2018; Sliz et al., 2018, 2020) has been built to determine terrestrial ages of meteorites. Doing so, the ^{14}C activity concentrations are measured in Bern and the ^{10}Be activity concentrations are measured at CEREGE (Aix-en-Provence, France; Arnold et al., 2010, 2013). Here, we present terrestrial ages for seven ordinary chondrite strewn fields and two single unpaired ordinary chondrites, all from Oman. The ages are determined via $^{14}C/^{10}Be$ ratios measured in purified silicate fractions. We anticipate that the data will help us to better understand the time scales of meteorite accumulation and losses in the deserts of Oman (and probably in a more general term also in other hot deserts).

INVESTIGATED SAMPLES

A summary of all relevant information of the studied strewn fields is given in Table 1. All materials used for this study come from the Omani-Swiss meteorite collection at the Natural History Museum in Bern. The location of strewn fields and individual samples is shown in Fig. 1, plots showing the position of individual analyzed stones of the strewn fields are shown in Fig. S1 in supporting information.

Dhofar (Dho) 005 is an L6 meteorite strewn field with poorly defined shape, located in the Dhofar region. Of the 706 recovered stones, 687 (125.5 kg) were reported by Grossman (2000) and 19 (6.0 kg) were collected during the Omani-Swiss search campaign 2001 (Fig. S1). Several ^{14}C terrestrial ages were reported by Al-Kathiri et al. (2005).

Dho 020 is a H4/5 meteorite strewn field with poorly defined shape, comprising more than 2000 individuals (256 kg; Grossman, 2000). An additional 78 individuals (1.29 kg) were collected during the Omani-Swiss search campaign in 2001. Our samples are from an accumulation of stones on an area of 0.9 × 0.7 km (Fig. S1b). A single ^{14}C age of 12.7 ± 1.3 ka was published by Al-Kathiri et al. (2005).

Jiddat al Harasis (*JaH*) *073* is an L6 ordinary chondrite strewn field with a length of 25.6 km (fall azimuth 340°). In total, 3463 individual stones (<1 g to 52.2 kg) were found (Fig. S1c). The total recovered mass is approx. 650 kg (Gnos et al., 2009). ^{14}C and ^{10}Be data were reported by Gnos et al. (2009) and Huber et al. (2008). Note, however, that Mészáros et al. (2018) already discussed that for JaH 073, the ^{14}C-^{10}Be terrestrial age is likely not reliable because ^{10}Be was probably not saturated at the time of fall. Huber et al. (2008) concluded that JaH 073 had a complex exposure history with a first-stage exposure under 2π conditions for ≤5 Ma followed by a second irradiation stage (4π) of 0.5–0.7 Ma. While the ^{10}Be data are a record of the first and the second irradiation stage, the ^{14}C data record only the second irradiation stage.

JaH 091 is an L5 ordinary chondrite strewn field with a length of 52.2 km (fall azimuth 126°), 702 recovered individuals, and a total meteorite mass of ~4500 kg (Gnos et al., 2006; Weber et al., 2017; Zurfluh et al., 2011) (Fig. S1). This makes JaH 091 the largest known strewn field in Oman. The sample measured in this study is from the first recovered individual (0210–0011; 123.37 kg). A single ^{14}C terrestrial age of 19.3 ± 1.3 ka and a cosmic ray exposure age of 15.7 ± 4.6 Ma were determined by, respectively, Al-Kathiri et al. (2005) and Leya et al. (2013). Weber et al. (2017) determined a preatmospheric radius of 100–130 cm using ^{26}Al.

Table 1. Information of the studied meteorite strewn fields (information as of June 16, 2020 from Meteoritical Bulletin Database, and OSMS database). The weathering grades (WG) are according to the weathering degree scales by Wlotzka (1993) and Zurfluh et al. (2016).

Meteorite	Date of find	Find location	Orientation and extent (km)	Type	WG (W)[a]	WG (W)[b] Mean	WG (W)[b] n[c]	Shock stage (S)	No. of individuals	Mass of largest individual (kg)	Total mass (kg)	CRE age (Ma)
Dho 005	March 6, 2000	Dhofar	Cannot be determined	L6	4	4.0	14	4	706	1.29	~131.5	ND
Dho 020	March 10, 2000	Dhofar	Unknown, ~12.5	H4-5	3	3.6	26	4	>2000	?	256	ND
JaH 073	January 17, 2002	Al Wusta	NW-SE, ~26.0	L6	2–4	3.5	24	4	3463	52.2	~650	≤5, 0.5–0.7[d]
JaH 091	October 19, 2002	Al Wusta	NW-SE, ~49.0	L5	3	3.5	83	2	703	1460	4600	15.7 ± 4.6[e]
SaU 001	March 16, 2000	Al Wusta	SW–NE, ~8.6	L4-5	1	1.8	5	2	1000	3.01	~423	ND
Shişr 015	February 2, 2001	Dhofar	W-E, ~24.7	L5	4	3.9	6	2	20	3.41	3.41	ND
RaS 418	February 5, 2010	Al Wusta	SW–NE, ~24.4	L6	4	3.9	8	5	16	30.8	69.1	ND

ND = not determined.
[a]Wlotzka (1993).
[b]Zurfluh et al. (2016).
[c]Number of thin sections studied for determination of the weathering degree.
[d]Huber et al. (2008)—first irradiation stage (2π), second irradiation stage (4π).
[e]Leya et al. (2013).

Sayh al Uhaymir (*SaU*) *001* (Fig. S1) is an L4/5 ordinary chondrite strewn field with thousands of individuals (408 kg) reported (Grossman, 2000). The strewn field has a length of ~8 km and a fall azimuth of ~235° (Korochantsev et al., 2003). One hundred and fifty-eight individuals with a mass of 14.8 kg were recovered during Omani-Swiss search campaigns. A single ^{14}C terrestrial age of 5.5 ± 1.3 ka was reported by Al-Kathiri et al. (2005).

SaU 163 is a single, unpaired H5 ordinary chondrite with a mass of 1.88 kg. The degree of weathering is W3.3. Bulk and leached ^{14}C activity concentrations were reported by Al-Kathiri et al. (2005), the latter indicating that SaU 163 is older than 50 ka. This meteorite was selected for our study to enable comparison with previous age data.

Shişr 015 is a strewn field with a length of 21.1 km (fall azimuth 265°) that consists of 43 individual stones with a total mass of 23.7 kg (OSMS database, Fig. S1). Available is a single ^{14}C terrestrial age of 36.5 ± 2.4 ka (Al-Kathiri et al., 2005).

Ramlat as Sahmah (*RaS*) *267* is a single, unpaired LL6 ordinary chondrite; the degree of weathering is W4.0. Zurfluh et al. (2016) measured a ^{14}C age of 30.5 ± 4.4 ka for a leached sample of RaS 267. This meteorite was selected in our study for comparison with previous age data.

Ramlat as Sahmah (*RaS*) *418* is an L6 ordinary chondrite strewn field (19.5 km length, fall azimuth 230°), with a total mass of 69.1 kg in 16 individual stones (Fig. S1). Neither the terrestrial age of RaS 418 has been previously determined nor have any other analyses of the strewn field been conducted.

EXPERIMENTAL METHODS

Carbon-14 Measurements at the University of Bern

Sample Preparation

Samples were milled and 1–2 g of the 125–200 μm grain size fractions was leached to remove terrestrial alteration products without affecting the primary minerals hosting the cosmogenic ^{14}C. A first leaching was done with 10 mL of 6.0 M hydrochloric acid for 30 min. After washing and drying, a second leaching was performed using monoethanolamine thioglycolate (EATG) 65% (Cornish & Doyle, 1984) for 48 h. All leaching steps were done at room temperature (approx. 24 °C). The leaching procedure primarily results in losses of oxidation products of metal and troilite, resulting in a sample enriched in silicates. Typically, a 50 mg sample of leached weathered chondrite corresponds to about 55 mg of bulk meteorite,

Table 2. Mass losses of metal and troilite in wt% for three strewn fields and the two unpaired individuals.

OC Type	H		L		LL
Sample	SaU 163	Dho 005	JaH 073	JaH 091	RaS 267
Correction (Fe loss wt%)	15.2	9.2	7.5	9.0	10.8
		Average	8.6		

These losses were determined in the leaching experiments described by Mészáros et al. (2018). For the correction of measured ^{14}C activity concentrations, only the loss of oxidized metal and troilite is considered because only these phases are a part of the unaltered bulk meteorite (Mészáros et al., 2018). The average mass correction value for L chondrites is used to correct the measured ^{14}C activity concentrations of samples for which no leaching experiments were performed (Dho 020, SaU 001, Shişr 015, and RaS 418), all of which are L chondrites.

containing most of the meteorite's cosmogenic ^{14}C. Correcting for such mass losses, we used the mean mass losses determined by Mészáros et al. (2018) (see also Table 2).

Carbon-14 Extraction and Accelerator Mass Spectrometry Measurements

The ^{14}C extraction procedure used in this work is described in detail in Sliz et al. (2020). All samples analyzed are ~50 mg aliquots. Briefly, the extraction procedure starts with preheating the sample at ~500 °C for 1 h in a continuous UHP O_2 flow with continuous pumping. Next, the crucible is disconnected from the vacuum pump, an O_2 partial pressure of 30 ± 5 mbar is established, and the temperature, that is, the generator current, is gradually increased. The evolved gases are expanded into a high-temperature gas purification furnace (Carbolite-Gero®) and collected in a metal helix that is cooled with liquid nitrogen (LN_2). The total extraction lasts for 10 min at ~1600 °C. After extraction, the crucible cools down, and any remaining O_2 gas can be safely pumped away. After the system is back to its minimum background pressure of below 5×10^{-4} mbar, the gas purification and CO_2 collection steps are carried out as described earlier by Mészáros et al. (2018). The gases collected in the helix are expanded into a known volume and the pressure is measured. Two gas cleaning steps are done: (i) using a water trap (−78 °C), removing any water that may be still in the system; and (ii) using a cold finger trap cooled with LN_2, to remove any gases other than CO_2, which is released when the trap's temperature is set to −100 °C. The released CO_2 gas is trapped in a glass capillary, cooled with LN_2. The collected CO_2 gas is expanded into a known volume above and including the capillary and the pressure is measured. If the amount of collected carbon is too low (<10 μg C) for a reliable $^{14}C/^{12}C$ measurement using the MICADAS system at the Department of Chemistry and Biochemistry, University of Bern, we add extra ^{14}C-free CO_2 (see also Mészáros et al., 2018). Whereas, when the amount of collected carbon is greater than 40 μg C, we expand the extracted CO_2 into a known volume and collect only a portion of the gas, for example, measurements of sample SaU001_243 (see Table S5 in supporting information).

The ^{14}C extraction of a sample consists of four measurements: (i) a system blank (BL)—a shot of ^{14}C-free CO_2 gas introduced into the extraction unit of the line. While no sample or blank material is processed, the heating of the crucible is as for samples and procedural blanks; (ii) procedural blank (AL)—a piece of aluminum used to wrap the meteorite aliquots is processed like a sample; (iii) sample extraction—an ~50 mg meteorite aliquot wrapped in Al-foil; and (iv) sample re-extraction—second measurement of the same meteorite aliquot. The carbon release for system and procedural blanks is typically 12–16 μg C and <1 μg C, respectively. Calibration of the system is via a pipette with a volume of ~1 cm^3. With a knowledge of volume and pressure (usually 25–30 mbar at room temperature), we can calculate the amount of carbon. Using now the known volume ratio of the pipette to the capillary (PIP/CAP) of 0.057, we can calculate the carbon amount (μg C) for any pressure measured in the capillary. The difference between the expected and the extracted CO_2 pressure is noted and is used to spot the first signs of malfunction in the system. Typically, the extracted and expected values agree within 3%. The carbon released during procedural blank measurements are one to two orders of magnitude lower than the carbon released in system blanks because they represent only the carbon extracted from a piece of Al-foil used for wrapping the samples. In this case, a spike of the ^{14}C-free CO_2 gas is added to the extracted gas to allow for a reliable accelerator mass spectrometry (AMS) measurement (see above). After the sample extraction, we always complete a sample re-extraction, which ensures that all of the carbon has been extracted from the sample. Although Mészáros et al. (2018) concluded that one extraction step is sufficient, at least for the JaH 073 samples they studied, we decided to always complete with a re-extraction step. For most meteorites (JaH 091, Dho 005, SaU 163, RaS 267, RaS 418), the second extraction yields blank levels. For some meteorites, and especially for some aliquots from some meteorites, the re-extractions yield higher ^{14}C (up to ~50% for one aliquot from SaU 001), indicating the first extraction was not sufficient to fully extract cosmogenic ^{14}C. The re-extractions are particularly important for meteorites

with short terrestrial ages and recently fallen meteorites, for which high ^{14}C yields are expected. Also, since the extraction unit is not emptied and cleaned after each sample, re-extractions prevent cross-contamination of samples and, thus, unreliable ^{14}C extractions. For the ^{14}C terrestrial age calculation, the ^{14}C extracted from the sample and the ^{14}C from the re-extraction are added together—after each has been corrected for blanks—to get the total ^{14}C extracted of the sample.

Measurements of the $^{14}C/^{12}C$ ratios were conducted using the MICADAS at the Laboratory for the Analysis of Radiocarbon with AMS (LARA) at the Department of Chemistry and Biochemistry, University of Bern (Szidat et al., 2014). For more information, see also Mészáros et al. (2018). In brief, glass ampules containing the collected CO_2 gas were introduced into the gas interface of the MICADAS, cracked open, the CO_2 gas was mixed with helium, and this mixture was transferred to the gas ion source. The ^{14}C results are expressed as $F^{14}C$ (fraction modern carbon) values.

Calculating ^{14}C Terrestrial Ages

For calculating the specific ^{14}C activity concentrations, we are using the ^{14}C data reduction equations given by Hippe et al. (2013) and Hippe and Lifton (2014). First, the absolute $^{14}C/^{12}C$ ratio is calculated using the measured fraction modern carbon ($F^{14}C$) and the $\delta^{13}C$ value. This ratio is then used to calculate the number of ^{14}C atoms (N_{14}). The N_{14} of sample and re-extraction are added so that the total ^{14}C from the two extractions are used for calculating the activity concentrations. Next, the total N_{14} is corrected for the procedural blank (AL; see Tables S1–S9 in supporting information; also see Mészáros et al., 2018) and then is used to calculate the activity concentration of the sample in dpm kg^{-1}. The calculated activity concentrations are corrected for metal and troilite loss during sample leaching (Table 2). Finally, the ^{14}C terrestrial age is calculated using the specific activity concentration of the samples (mass-corrected ^{14}C in Table 3) and the saturation activity of the studied meteorite type. For a detailed description of the data reduction calculations, see also Mészáros et al. (2018).

Beryllium-10 Sample Preparation at CEREGE and Measurements at the ASTER AMS

Chemical extractions and AMS measurements of ^{10}Be were performed at CEREGE and the ASTER AMS facility, Aix-en-Provence, France. One to four 200 mg aliquots of each sample were analyzed. Samples spiked with ^{9}Be (100 mg of a 3025 ± 9 ppm in-house solution) were dissolved in 10 mL of 22 M HF for 2–4 days. Residues were treated with 1 mL nitric acid (HNO_3, 1 M), a small amount of Milli-Q® water, and was centrifuged. The solutions were dried at 150 °C. Be was extracted by successive solvent extractions and alkaline precipitations following the procedure described by Bourlès (1988) and Brown et al. (1991). AMS targets were prepared from the resulting BeO powder. Doing so, sample BeO was mixed with niobium (Nb) powder (Aldrich, 325 mesh, 99.8%) in a 1:1.5 ratio before being loaded into the AMS cathodes (Arnold et al., 2010). The mixed powder was pressed into the cathodes by applying 250 kg for 30 s. In total, we prepared 40 samples and one blank.

For most samples, solid residues were left after the HF and HNO_3 dissolution steps. Several of these solids were analyzed at CEREGE by X-ray diffraction using a Panalytical X'Pert PRO X-ray diffractometer equipped with a Cobalt source (λ = 1.79 Å) running at 40 kV and 40 mA. Each sample was scanned from 5° to 75° (2θ) with a step size of 0.033° at a total counting time of 2 h. After grinding in an agate mortar, the samples were deposited on low background silicon plates with a drop of ethanol to make a thin and homogeneous powdered layer. Samples were also spun at 15 rpm during measurement to improve statistics. The identification of the crystallized compounds was performed using the ICDD PDF2 database. All solid residues gave very similar X-ray diffraction spectra, showing almost exclusively fluoride compounds in the form of $KNiCrF_6$ and MgF_2. For MgF_2, a slight shift of the peaks was observed, which we attribute to a substitution of the Mg by other cations. In addition, one sample may contain small amounts of magnetite. No traces of initial main minerals (olivine, pyroxene, plagioclase) have been detected. From this result, we can safely conclude that all ^{10}Be in the samples was extracted during the dissolutions. To this end, ^{10}Be measurements were normalized by the initial sample mass rather than the dissolved mass (initial mass minus mass of precipitates).

A detailed description of the ASTER 5 MV AMS facility is given by Arnold et al. (2010, 2013). Together with the unknown samples, the standard reference material NISTSRM4325 (with an assumed $^{10}Be/^{9}Be$ ratio of $[2.79 \pm 0.03] \times 10^{-11}$; Nishiizumi et al., 2007) and machine blanks were run. The measured $^{10}Be/^{9}Be$ ratios are corrected for procedural blanks and the specific ^{10}Be activity concentrations in dpm kg^{-1} are calculated.

Uncertainties of the ^{14}C and ^{10}Be Measurements and Data

The potential sources of uncertainties are multiple, for example, day-to-day variations in operation of the ^{14}C extraction line and the AMS facilities and operator-specific variations in following the extraction protocols.

Table 3. ^{14}C and ^{14}C-^{10}Be terrestrial ages of the measured strewn field samples and two single meteorites. The data are presented in chronological order.

Sample	Internal Nr.	Measured ^{14}C (dpm kg^{-1})	Mass corrected ^{14}C (dpm kg^{-1})	Measured ^{10}Be (dpm kg^{-1})	T_{14} (ka)	$T_{14/10}$ (ka)	Reference
JaH 073[a,b,c]	0201-640	5.89 ± 0.36	5.45 ± 0.33	14.9 ± 0.2[e]	18.4 ± 2.8[g]	15.9 ± 2.9[g,h]	This study
JaH 073 (JaH073_5)[a,d]	0201-640	6.05 ± 0.12	5.27 ± 0.10		18.7 ± 2.8[g]	16.2 ± 2.6[g,h]	This study
				Mean age	18.6 ± 2.0	16.1 ± 2.0	
JaH 073 (JaH073_018)[a]	0201-640	6.50 ± 0.09	6.02 ± 0.08		17.6 ± 0.4[g]	14.5 ± 2.5[g,h]	Mészáros et al. (2018) (^{14}C); this study (^{10}Be)
JaH 073 (JaH073_019)[a]	0201-640	6.34 ± 0.09	5.87 ± 0.08		17.8 ± 0.4[g]		
JaH 073	0201-640	5.76 ± 0.12			18.0 ± 1.3	15.4 ± 0.4	Al-Kathiri et al. (2005) (^{14}C); Gnos et al. (2009) (^{10}Be)
JaH 073	0201-592	4.75 ± 0.09			19.6 ± 1.3	12.8 ± 0.4	Al-Kathiri et al. (2005) (^{14}C); Gnos et al. (2009) (^{10}Be)
JaH 073	0201-821	3.79 ± 0.11			21.5 ± 1.3	15.0 ± 0.4	Al-Kathiri et al. (2005) (^{14}C); Gnos et al. (2009) (^{10}Be)
JaH 073	0201-664	12.8 ± 0.14			11.4 ± 1.3	8.28 ± 0.37	Gnos et al. (2009)
JaH 073	0201-642	49.9 ± 0.32			0.2 ± 1.3	Recent	Gnos et al. (2009)
Shişr 015 (Shisr015_78_001)[a,c]	0301-78	1.11 ± 0.07	1.02 ± 0.06	17.6 ± 0.1[f]	32.2 ± 3.9[g]	30.9 ± 3.2[g,h]	This study
Shişr 015 (Shisr015_78_002)[a,c]	0301-78	1.17 ± 0.07	1.07 ± 0.06		31.8 ± 3.8[g]		This study
Shişr 015 (Shisr015_165_001)[a,c]	0102-165	1.25 ± 0.07	1.15 ± 0.06	17.0 ± 0.2	31.2 ± 3.8[g]	29.7 ± 3.1[g,h]	This study
Shişr 015 (Shisr015_165_002)[a,c]	0102-165	1.29 ± 0.06	1.18 ± 0.05		31.0 ± 3.8[g]		This study
Shişr 015 (Shisr015_1942_001)[a,c]	0212-1942	0.84 ± 0.06	0.76 ± 0.05	15.4 ± 0.2	34.6 ± 4.1[g]	32.5 ± 3.3[g,h]	This study
Shişr 015 (Shisr015_1942_002)[a,c]	0212-1942	0.82 ± 0.04	0.75 ± 0.04		34.7 ± 4.1[g]		This study
				Mean age	32.5 ± 1.6	31.0 ± 1.9	
Shişr 015	0102-165	0.6 ± 0.2			36.5 ± 2.4		Al-Kathiri et al. (2005) (T_{14}); Zurfluh et al. (2016) (^{14}C)
JaH 091 (JaH091_002)[a,c]	0210-11	11.9 ± 0.2	10.9 ± 0.2	17.7 ± 0.2[e]	12.7 ± 2.3[g]	10.9 ± 1.7[g,h]	This study
JaH 091 (JaH091_003)[a,c]	0210-11	13.9 ± 0.2	12.7 ± 0.2		11.5 ± 3.1[g]		This study
				Mean age	12.3 ± 1.9		
JaH 091	0210-11	4.9 ± 0.1			19.3 ± 1.3		Al-Kathiri et al. (2005) (T_{14}); Zurfluh et al. (2016) (^{14}C)

Table 3. *Continued.* ^{14}C and ^{14}C-^{10}Be terrestrial ages of the measured strewn field samples and two single meteorites. The data are presented in chronological order.

Sample	Internal Nr.	Measured ^{14}C (dpm kg^{-1})	Mass corrected ^{14}C (dpm kg^{-1})	Measured ^{10}Be (dpm kg^{-1})	T_{14} (ka)	$T_{14/10}$ (ka)	Reference
Dho 020 (Dho020_90_001)[a,c]	0101-90	9.11 ± 0.20	8.33 ± 0.18	18.6 ± 0.2	14.1 ± 2.4[g]	13.2 ± 1.8[g,h]	This study
Dho 020 (Dho020_90_002)[a,c]	0101-90	10.64 ± 0.21	9.71 ± 0.19		12.8 ± 2.3[g]		This study
Dho 020 (Dho020_79_001)[a,c]	0101-79	9.25 ± 0.20	8.47 ± 0.18	17.4 ± 0.2	13.9 ± 2.4[g]	13.5 ± 1.8[g,h]	This study
Dho 020 (Dho020_79_002)[a,c]	0101-79	9.26 ± 0.19	8.46 ± 0.17		13.9 ± 2.4[g]		This study
Dho 020 (Dho020_71_001)[a,c]	0101-71	8.60 ± 0.19	7.86 ± 0.17	16.9 ± 1.3[f]	13.5 ± 2.6[g]	14.3 ± 1.9[g,h]	This study
Dho 020 (Dho020_71_002)[a,c]	0101-71	7.82 ± 0.15	7.15 ± 0.14		15.3 ± 2.5[g]		This study
				Mean age	13.9 ± 1.0	13.6 ± 1.1	
Dho 020	0101-052				12.7 ± 1.3		Al-Kathiri et al. (2005)
SaU 001 (SaU001_290_001)[a,c]	0201-290	42.1 ± 0.5	38.6 ± 0.5	8.3 ± 0.1	2.3 ± 1.60[g]	(−4.8) ± 0.7[g,h]	This study
SaU 001 (SaU001_290_002)[a,c]	0201-290	35.8 ± 0.5	32.7 ± 0.5		3.7 ± 1.7[g]		This study
SaU 001 (SaU 001_243_001)[a,c]	0201-243	14.2 ± 0.2	13.0 ± 0.2	8.8 ± 0.1	11.3 ± 2.2[g]	6.8 ± 2.6[g,h]	This study
SaU 001 (SaU 001_243_002)[a,c]	0201-243	7.5 ± 0.2	6.9 ± 0.2		16.5 ± 2.6[g]		This study
SaU 001 (SaU 001_04_001)[a,c]	0201-04	17.1 ± 0.4	15.7 ± 0.4	9.3 ± 0.2[f]	9.7 ± 2.1[g]	5.7 ± 2.5[g,h]	This study
SaU 001 (SaU 001_04_002)[a,c]	0201-04	9.3 ± 0.3	8.5 ± 0.3		14.8 ± 2.5[g]		This study
				Mean age	7.8 ± 2.3	6.3 ± 1.5[k]	
SaU 001	0102-218	26.3 ± 0.2			5.5 ± 1.3		Al-Kathiri et al. (2005) (T_{14})
Dho 005 (Dho005_001)[a,c]	0102-200	0.72 ± 0.03	0.66 ± 0.03	14.6 ± 0.1[e]	35.8 ± 4.1[g]	35.4 ± 2.5[g,h]	This study
Dho 005 (Dho005_002)[a,c]	0102-200	0.40 ± 0.02	0.36 ± 0.02		40.8 ± 4.5[g]		This study
				Mean age	38.1 ± 3.0		
Dho 005	0102-179	0.75 ± 0.14[i]			34.6 ± 2.0[i]		Al-Kathiri et al. (2005)
Dho 005	0102-200	0.37 ± 0.13[i]			40.6 ± 3.1[j]		Al-Kathiri et al. (2005)
Dho 005	0102-205	0.56 ± 0.10[i]			37.4 ± 2.0[j]		Al-Kathiri et al. (2005)
SaU 163 (SaU163_001)[a,c]	0101–002	3.30 ± 0.05	2.80 ± 0.04	19.5 ± 0.1[e]	23.0 ± 3.1[g]	23.3 ± 2.0[g,h]	This study
SaU 163 (SaU163_002)[a,c]	0101–002	3.52 ± 0.06	3.99 ± 0.05		22.5 ± 3.1[g]		This study
				Mean age	22.8 ± 2.2		
SaU 163	0101–002	3.56 ± 0.15			21.2 ± 1.3		Al-Kathiri et al. (2005)
	0101–002	(−0.47) ± 0.20 (leached)			>50		

Table 3. *Continued.* ^{14}C and ^{14}C-^{10}Be terrestrial ages of the measured strewn field samples and two single meteorites. The data are presented in chronological order.

Sample	Internal Nr.	Measured ^{14}C (dpm kg^{-1})	Mass corrected ^{14}C (dpm kg^{-1})	Measured ^{10}Be (dpm kg^{-1})	T_{14} (ka)	$T_{14/10}$ (ka)	Reference
RaS 267 (RaS267_001)[a,c]	0801–005	2.53 ± 0.05	2.25 ± 0.04	14.4 ± 0.1[e]	26.3 ± 3.3[g]	23.0 ± 2.0[g,h]	This study
RaS 267 (RaS267_002)[a,c]	0801–005	2.50 ± 0.05	2.22 ± 0.04		26.4 ± 3.4[g]		This study
				Mean age	26.3 ± 2.4		
RaS 267	0801–005		1.4 ± 0.7[j]		30.5 ± 4.4		Zurfluh et al. (2016)
RaS 418 (RaS 418_153_001)[a,c]	1002–153	2.76 ± 0.05	2.52 ± 0.05	19.0 ± 0.2	24.8 ± 3.3[g]	24.5 ± 2.1[g,h]	This study
RaS 418 (RaS 418_153_002)[a,c]	1002–153	2.61 ± 0.05	2.43 ± 0.05		25.1 ± 3.3[g]		This study
RaS 418 (RaS 418_32_001)[a,c]	1201–32	3.02 ± 0.05	2.76 ± 0.05	19.5 ± 0.3	24.0 ± 3.2[g]	24.0 ± 2.1[g,h]	This study
RaS 418 (RaS 418_32_002)[a,c]	1201–32	2.85 ± 0.05	2.61 ± 0.05		24.5 ± 3.2[g]		This study
				Mean age	24.6 ± 1.6	24.2 ± 1.5	

All uncertainties are 1σ + 1.3 ka.
[a]Preheated leached sample.
[b]Based on four ^{14}C measurements of JaH 073.
[c]Measured using RF heating + Pt-crucible.
[d]Measured using RF heating + Fe-pellets.
[e]Based on four ^{10}Be measurements of a homogenous ground sample.
[f]Based on two ^{10}Be measurements of a homogenous ground sample.
[g]Saturation of ^{14}C assumed to be 46.0, 51.1, and 55.2 dpm kg^{-1} for H, L, and LL chondrites, respectively.
[h]Saturation of ^{10}Be assumed to be 20.6 and 22.1 dpm kg^{-1} for H and L/LL chondrites, respectively.
[i]Bulk activity/T_{14}.
[j]Leached activity/T_{14}—samples treated with ethanolamine thioglycolate prior to ^{14}C analysis.
[k]Mean age for SaU 001 calculated by excluding sample 290.

For the AMS data, many uncertainties are already accounted for in the given data. For example, the MICADAS AMS system accounts for all possible sources of uncertainties, including counting statistics, uncertainties from blank subtraction, standard normalization, and correction for isotope fractionation. In addition, the data include a 1.5‰ systematic uncertainty covering the day-to-day variability (Szidat et al., 2014). Consequently, the given AMS ^{14}C data already include all possible sources for statistical and systematic uncertainties. The same applies to the ^{10}Be data from the ASTER AMS; the raw data already include measurement uncertainties (statistical), the uncertainty of the standard, the uncertainty of the mean of the standard measurement (instrumental), and a systematic uncertainty of ~0.5% (Arnold et al., 2010).

For estimating the reproducibility of the ^{14}C extraction procedure, Sliz et al. (2020) used a homogenized ground sample from the L6 chondrite JaH 073. Based on four replicate measurements, they found a resultant 1σ standard deviation of 2.0×10^6 atoms ^{14}C per g, which is 7.8%. We therefore added a systematic uncertainty of ±7.8% to the measured ^{14}C atoms per gram of meteorite. We assume that this approach is valid for meteorites with terrestrial ages in the range 0–20 ka, that is, for specific ^{14}C activity concentrations in the range (20–70) × 10^6 atoms per g. Note that the repeated analysis of the JaH 073 samples (in total seven) cannot be used to determine the external reproducibility because the extraction protocols varied: (i) extraction using a convection oven (JaH073_018 and JaH073_019; Mészáros et al., 2018), (ii) extraction using an RF generator and Fe pellets as "combustion catalysts" (JaH073_5; Sliz et al., 2020), and (iii) extraction using an RF generator and Pt-crucible as the heat medium via induction heating (JaH073_012, JaH073_013, JaH073_016, JaH073_017; Table S1) (Sliz et al., 2020). Hence, the reproducibility estimate is based only on the replicates measured using the updated extraction protocol.

Calculating ^{14}C-^{10}Be Terrestrial Age

The ^{14}C-^{10}Be terrestrial ages are calculated using:

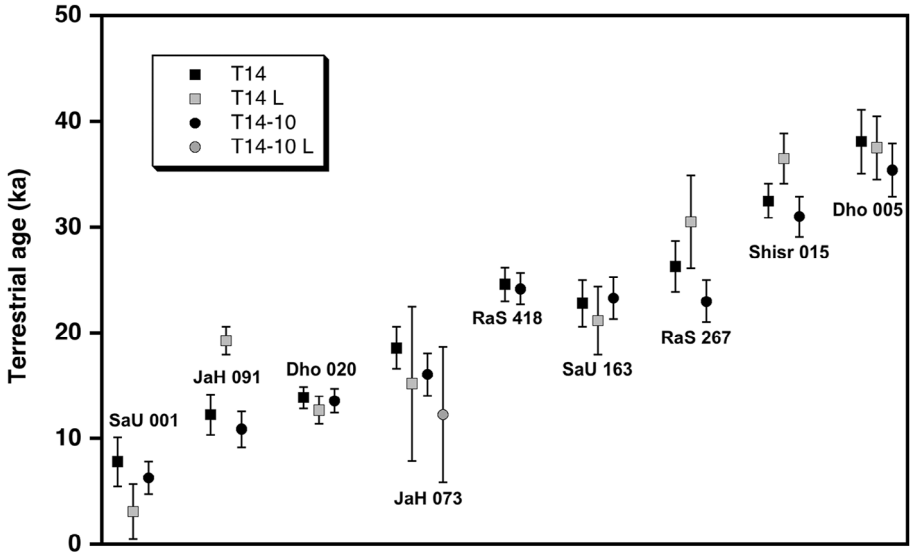

Fig. 2. Plot showing a comparison of measured and published ^{14}C and ^{14}C-^{10}Be terrestrial ages for the studied samples. T14 is the mean of ^{14}C ages obtained in this study; T14 L is the mean of ^{14}C literature data (one age of >50 ka for SaU 163 omitted); T14-10 is the mean of ^{14}C-^{10}Be ages obtained in this study; T14-10 L is the mean of ^{14}C-^{10}Be literature data (only JaH 073).

$$T_{\frac{14}{10}} = \frac{1}{(\lambda_{10}-\lambda_{14})} \ln\left(\frac{\left(\frac{A_{14}}{A_{10}}\right)_m}{\left(\frac{A_{14}}{A_{10}}\right)_s}\right) \quad (1)$$

where $\left(\frac{A_{14}}{A_{10}}\right)_m$ is the measured activity ratio of ^{14}C and ^{10}Be and $\left(\frac{A_{14}}{A_{10}}\right)_s$ is the $^{14}C/^{10}Be$ ratio of saturation activities. For the ^{14}C saturation activities, we use 46.0 ± 1.0 dpm kg^{-1} for H chondrites, 51.1 ± 1.0 dpm kg^{-1} for L chondrites, and 55.2 ± 1.0 dpm kg^{-1} for LL chondrites (Jull, Cielaszyk et al., 1998). For ^{10}Be, the saturation activities are 20.6 ± 1.0 dpm kg^{-1} for H chondrites and 22.1 ± 1.0 dpm kg^{-1} for L and LL chondrites (e.g., Jull et al., 2013). From this, we calculate $^{14}C/^{10}Be$ production rate ratios of 2.23 ± 0.19 for H chondrites, 2.31 ± 0.19 for L chondrites, and 2.50 ± 0.20 for LL chondrites. However, the $^{14}C/^{10}Be$ production rate ratio is not expected to vary significantly with chemical composition, that is, with meteorite type, as both isotopes are mainly produced from oxygen. Therefore, the calculated variations are most likely due to the use of average and sometime inconsistent production rates. For example, the model of Leya and Masarik (2009) shows that the $^{14}C/^{10}Be$ production rate ratio varies only by 1%–3% between H- and LL chondrites. We therefore used a constant production rate ratio of 2.5 ± 0.2 for calculating the ^{14}C-^{10}Be ages. The decay constants for ^{10}Be and ^{14}C are, respectively, $\lambda_{10} = 4.997 \times 10^{-7}$yr^{-1} (based on the accepted half-life of 1.387×10^6 yr; Korschinek et al., 2010) and $\lambda_{14} = 1.216 \times 10^{-4}$yr^{-1} (based on the accepted half-life of 5700 ± 30 yr; National Nuclear Data Center, Brookhaven National Laboratory). The ^{14}C-^{10}Be terrestrial age dating method used here assumes that the $^{14}C/^{10}Be$ production rate ratio is independent of shielding. While this might not entirely be true, especially not for large strewn field meteorites studied here, we follow the usual procedure of Jull et al. (2013) and add a systematic uncertainty of ± 1.3 kyr to the calculated ^{14}C and ^{14}C-^{10}Be terrestrial ages, which corresponds to a total uncertainty of ~15% in the $^{14}C/^{10}Be$ production rate ratio.

RESULTS AND DISCUSSION

Data for Individual Strewn Fields and Meteorites

The ^{14}C and ^{10}Be activities and the calculated terrestrial ages are given in Table 3 and Fig. 2. In Tables S1–S9, the raw ^{14}C data are compiled in chronological order to demonstrate how the performance of the ^{14}C extraction line, that is, the system and procedural blanks, developed. The measured ^{10}Be data for all samples are given in Table S10 in supporting information. In the following discussion, we are using a shorter version for the sample numbers, for example, we are using only 640 instead of the complete number 0201-640. In the data tables, we are giving the full reference numbers (Table 3; Table S1). Also, when discussing the

degree of sample weathering, we use the scale established by Zurfluh et al. (2016). Note that all averages given below are weighted averages, using the uncertainties as weights.

Jiddat al Harasis 073

The homogenized powder from an individual stone (640) of the JaH 073 meteorite strewn field is our reference sample, used to test the performance of the ^{14}C extraction line as described by Sliz et al. (2020). Table S1 compiles the data of four measurements done using two different RF coil setups. Some of the results were previously discussed by Sliz et al. (2020). The major finding is that the reproducibility of the measurements is satisfactory. Table 3 compiles the calculated ^{14}C and $^{14}C/^{10}Be$ terrestrial ages and shows a comparison with literature data. Considering only data from our group, the mass-corrected ^{14}C activity concentrations range from 5.26 to 6.02 dpm kg^{-1}, that is, the variability is ~14%. The average value is (5.75 ± 0.18) dpm kg^{-1}, that is, the 1σ standard deviation is 3.1%. We consider this a good reproducibility considering that the data have been obtained by different operators and on an extraction line that has been significantly changed and improved over the years. The new data are also in good agreement with literature data for the same individual (Al-Kathiri et al., 2005). There is a significant discrepancy to data from other stones (642 and 664). Gnos et al. (2009) concluded that the stones are likely to have been contaminated with terrestrial carbonates as the high ^{14}C content correlates with large amounts of carbon in the samples. However, this interpretation is not as straightforward as one would like it to be. For example, sample 821, which has a low specific ^{14}C activity concentration, shows a higher degree of weathering (W4.5; based on the refined weathering scale by Zurfluh et al., 2016) than stone 642 (W3.6; Zurfluh et al., 2016), which has the highest ^{14}C activity concentration. If the discrepancy were due to contamination, we would expect the highly weathered sample to contain more terrestrial carbonates and contamination, hence having a higher ^{14}C activity concentration. The terrestrial age calculated from the two analyses in this study is 18.6 ± 2.0 ka. By including two previous analyses from our group (Mészáros et al., 2018) (Table 3), the mean activity concentration for ^{14}C of four analyses is 5.75 ± 0.18 dpm kg^{-1} corresponding to a ^{14}C terrestrial age of 18.1 ± 2.7 ka, used as the best estimate for the terrestrial age of JaH 073.

Four ^{10}Be measurements of a homogenized ground sample of JaH 073 were performed. The measured ^{10}Be activity concentrations average at 14.9 ± 0.2 dpm kg^{-1}. So far we determined ^{14}C-^{10}Be terrestrial ages for only one stone (640) of the JaH 073 strewn field. The values of 15.3 ± 3.4 ka and 15.5 ± 2.9 ka, determined from the same homogenized sample powder using two independent ^{14}C measurements but the same value for ^{10}Be, are slightly lower than our best estimate for the ^{14}C terrestrial age. However, as already mentioned, JaH 073 has a complex exposure history (Huber et al., 2008). By way of example, assuming a second irradiation stage of 0.7 Ma (Huber et al., 2008), the ^{10}Be activity concentration from this second stage is expected to be ~70% lower than the activity concentration at saturation. With a saturation activity concentration of 22.1 dpm kg^{-1}, this would correspond to ~6.6 dpm kg^{-1}, that is, far lower than 17.6–19.1 dpm kg^{-1} measured by us. Consequently, a significant part of the measured ^{10}Be concentration is from the first 2π irradiation stage.

Shişr 015

The ^{14}C-^{10}Be ages of the Shişr 015 strewn field were already discussed by Sliz et al. (2019). Those ages marginally differ from the ones presented here because previously only the number of ^{14}C atoms extracted during the major extraction was considered. Here, we use the total number of extracted ^{14}C atoms, that is, major extraction plus re-extraction. Consequently, previously calculated ^{14}C activity concentrations were slightly too low, resulting in slightly higher ^{14}C and ^{14}C-^{10}Be terrestrial ages. The updated ages and ^{14}C data are given in Tables 3 and S2, respectively. Three individuals of Shişr 015 were measured, with two replicates per sample. The mass-corrected ^{14}C activity concentrations range from 0.75 to 1.18 dpm kg^{-1} (Table 3). The average value is (0.95 ± 0.08) dpm kg^{-1}, that is, the 1σ standard deviation is ~8%. The variability for individual stones ranges from ~1% to ~5%. The calculated ^{14}C ages range from 31.0 ± 3.8 to 34.7 ± 4.1 ka with an average value of 32.5 ± 1.6 ka. The previously reported ^{14}C terrestrial age (Al-Kathiri et al., 2005) of 36.5 ± 2.4 ka for stone 165 is slightly higher than the ones measured by us for the same sample, 31.0 ± 3.8 ka and 31.2 ± 3.8 ka. The discrepancy can result from slightly different sample preparation procedures used for both studies. Al-Kathiri et al. (2005) stated that their samples were prepared according to protocols given in Jull et al. (1989, 1990, 1993) and Jull, Cielaszyk et al. (1998) where leaching using phosphoric acid (H_3PO_4) is performed.

Four ^{10}Be measurements were performed for three different Shişr 015 individuals: two replicates of stone 78, one sample from stone 165, and one sample from stone 1942. The ^{10}Be activity concentrations range from 15.4 to 17.6 dpm kg^{-1}, that is, they agree within ~19%. The average value is 16.7 dpm kg^{-1} with a 1σ standard

deviation of 6.8%. The calculated ^{14}C-^{10}Be terrestrial ages for the individual stones 78, 165, and 1943 are 30.9 ± 3.2 ka, 29.7 ± 3.1 ka, and 32.5 ± 3.3 ka, respectively. The determined ages agree within their uncertainties, hence confirming that they belong to the same fall. The ^{14}C-^{10}Be ages have a variability of only 9%, whereas the variability of ^{14}C-only ages is 12%. Thus, we also confirm that ^{14}C-^{10}Be terrestrial ages are more reliable than ^{14}C-only ages. The average ^{14}C-^{10}Be age for Shişr 015 is 31.0 ± 1.9 ka, which we define as the best estimate of the terrestrial age for this strewn field.

Jiddat al Harasis 091

Table S3 compiles the ^{14}C data of three replicate measurements of a homogenized ground sample from the JaH 091 strewn field. Unfortunately, one sample was lost during the AMS measurement; hence, only two successful measurements can be used for discussion. The ^{14}C activity concentrations agree within 16%. The ^{14}C terrestrial ages of 12.7 ± 2.3 ka and 11.5 ± 3.1 ka (Table 3) are significantly lower than the age of 19.3 ± 1.3 ka reported earlier by Al-Kathiri et al. (2005) for the same sample. The source of the discrepancy is unclear. We calculate a mean ^{14}C age for JaH 091 of 12.3 ± 1.9 ka.

Four aliquots of a homogenized ground sample of JaH 091 were measured for ^{10}Be, yielding an average ^{10}Be activity concentration of 17.7 ± 0.2 dpm kg^{-1}. Leya et al. (2013) measured a cosmic ray exposure age of JaH 091 of 15.7 ± 4.6 Ma, which means that ^{10}Be was likely in saturation at the time of fall. The calculated ^{14}C-^{10}Be age of 10.9 ± 1.7 ka, taken as best estimate age for the strewn field, is in reasonable agreement with the ^{14}C age of 12.3 ± 1.9 ka. Optically stimulated luminescence (OSL) ages of 15.2 ± 1.4 and 18.6 ± 1.5 ka for soils below two large fragments reported by Zurfluh et al. (2011) indicate soil stability before the fall event.

Dhofar 020

Table S4 summarizes the ^{14}C data of the three measured Dho 020 samples. Two ^{14}C activity concentrations were measured per sample, resulting in six data points. The reproducibility is ~16% for stone 90, ~1% for stone 79, and ~10% for stone 71 (Table S4). By averaging the ^{14}C activity concentrations for the individual stones, we calculate ^{14}C ages in the range 13.4 ± 1.7 ka to 14.4 ± 1.8 ka for the three samples (mean 13.9 ± 1.0 ka), that is, the variability is ~7%. Considering the advanced degree of weathering (W 3.6) of Dho 020, the ages are quite low. The published ^{14}C age of 12.7 ± 1.3 ka for stone 52 (Al-Kathiri et al., 2005) is somewhat lower than our new ages; however, all ages agree with the published age within their uncertainties. Again, the slight discrepancy could result from the different sample preparation procedures.

Four ^{10}Be replicates were measured for Dho 020; two of stone 71, one of stone 79, and one of stone 90. The measured ^{10}Be ranges from 16.9 to 18.6 dpm kg^{-1}. The two ^{10}Be activity concentrations for stone 71 agree within ~8%, which is slightly outside the analytical uncertainties. The calculated ^{14}C-^{10}Be ages are 13.2 ± 1.8 ka, 13.5 ± 1.8 ka, and 14.3 ± 1.9 ka for samples 90, 79, and 71, respectively. The average ^{14}C-^{10}Be age for Dho 020 is 13.6 ± 1.1 ka (taken as best estimate age for the strewn field).

Sayh al Uhaymir 001

Three samples of SaU 001 (04, 243, and 290) were studied for ^{14}C (Table S5) and ^{10}Be. For ^{14}C, we performed two measurements per sample, resulting in six data points. For ^{10}Be, we measured two aliquots for stone 04, and one aliquot each for stones 290 and 243. The variability of the two ^{14}C measurements performed for each aliquot is ~18%, ~90%, and ~84% for sample 290, 243, and 04, respectively, that is, the reproducibility for samples 243 and 04 is bad. Interestingly, the ^{14}C activity concentrations also vary significantly among the studied samples. For example, while the ^{14}C activity concentrations for sample 290 vary by ~18%, they are both significantly higher than the four ^{14}C activity concentrations measured for the other two samples. Considering the good reproducibility of all measurements performed in this study, the observed variability among the different samples is likely not caused by analytical artifacts. The important finding therefore is that the variability among the different stones is much larger than the variability among the different samples of the same stone. The average ^{14}C activity concentrations are (35.7 ± 1.3) dpm kg^{-1}, (10.0 ± 1.4) dpm kg^{-1}, and (11.1 ± 1.9) dpm kg^{-1}, for stones 290, 243, and 04, respectively. The thus calculated average ^{14}C ages for the three stones have also a significant spread between 3.0 ± 1.2 ka and 13.5 ± 1.7 ka. The (weighted, using the uncertainties as weights) mean ^{14}C terrestrial age of SaU 001 is 7.8 ± 2.3 ka.

The majority of the weathering proxies studied by Al-Kathiri et al. (2005) indicate a terrestrial age of less than 15 ka for SaU 001. The same authors give a ^{14}C terrestrial age of 5.5 ± 1.3 ka for stone 218 (W2). Most of our measured ages are higher and it is likely that other factors are at play than just differences in sample preparation procedures. As already mentioned above, there is a reasonable agreement for the different aliquots of the same stone but a significant difference

among the various stones. These discrepancies could be attributed to the previously mentioned variability in weathering degree among the different stones of the strewn field, ranging from W1 to W3. Al-Kathiri et al. (2005) conclude that temporary burial and/or specific local surface morphology (e.g., accumulation of water in depressions) could result in intensified weathering and consequently in an excess in the contributions of terrestrial contamination in some samples. However, the studied samples are unlikely to contain significant amounts of terrestrial contamination, increasing ^{14}C activity concentrations, and thereby lowering their ^{14}C terrestrial ages because our sample preparation procedure has been proven to efficiently remove terrestrial contamination (Mészáros et al., 2018). However, the system and procedural blanks show an increase in N_{14} by up to a factor of 10 over the course of the SaU 001 measurements. Interestingly, the extraction of sample 243 gave an atypically high pressure of the extracted gas, which was initially interpreted as water and/or contamination to be removed during the gas cleaning. However, it was not like this; the CO_2 pressures from sample 290 were 1.3 mbar (290_001) and 2.0 mbar (290_002), whereas sample 243 gave CO_2 pressures of 5.6 mbar (243_001) and 6.3 mbar (243_002). For sample 04, which has a high ^{14}C content, the re-extraction contributed ~50% to the total ^{14}C, that is, the extraction was by far not complete and this was exceptionally worse for this sample. It is clear that the high CO_2 content was not due to a degassing crucible, which would have been observed in the system and procedural blanks. In addition, given that sample 243 has moderate ^{14}C activity concentrations of 11.8 and 14.6 dpm kg^{-1}, the unusually high CO_2 pressures are unlikely to result from contamination by terrestrial carbonates, which would have elevated the measured activity concentrations. For now, it remains unclear why the two aliquots of sample 243 produced such an increased CO_2 pressure.

It is clear, however, that SaU 001 has a short terrestrial age, that is, we expect high ^{14}C activity concentrations. For such young samples, re-extractions are especially important to fully extract all ^{14}C and to avoid cross-contamination between samples from different meteorites but also between aliquots of the same meteorite. Before the SaU 001 measurements, the extraction system had performed trouble-free and with a good reproducibility in terms of blanks but also in terms of sample measurements. However, before SaU 001, the crucible was already filled with 12 samples plus 12 aluminum foils, which might have rendered heating less efficient and thereby given too low ^{14}C activity concentrations. After the SaU measurements, the Pt-crucible was replaced.

The ^{10}Be activity concentrations range from 8.3 to 9.3 dpm kg^{-1} for the three SaU 001 samples, that is, the variability is only 5.7%, far lower than the variability for the ^{14}C activity concentrations. The average ^{10}Be activity concentration is 8.8 dpm kg^{-1} with a 1σ standard deviation of 6.0%. The calculated ^{14}C-^{10}Be ages are (−4.8) ± 0.7 ka, 6.8 ± 2.6 ka, and 5.7 ± 2.5 ka for samples 290, 243, and 04, respectively. Note that a negative age is impossible. Though the ^{10}Be data are all consistent, they are surprisingly low, not only compared to the saturation activity but also relative to the ^{10}Be data for the other studied meteorites, that is, especially for the L5 strewn field JaH 091. To be more precise, the average ^{10}Be activity concentration for SaU 001 is about two times lower than for JaH 091. Note that JaH 091 has a cosmic ray exposure age of ~15 Ma, that is, sufficient for ^{10}Be being in saturation (Leya et al., 2013). The low ^{10}Be activity concentrations of SaU 001 can either be due to a very large pre-atmospheric size, which is unlikely considering the relatively high ^{14}C activity concentrations, or it can be due to a short and/or complex exposure history. To fully understand the history of SaU 001 and the status of ^{10}Be saturation, noble gas data would be needed. Given the current lack of knowledge about SaU 001's cosmic ray exposure history, we use the mean ^{14}C terrestrial age of 7.8 ± 2.3 ka as the best estimate of the strewn field's terrestrial age.

Dhofar 005

Previously published ^{14}C terrestrial ages of Dho 005 are 37.4 ± 2.0 ka, 34.6 ± 2.0 ka, and 40.6 ± 3.1 ka (Al-Kathiri et al., 2005) for bulk samples of stones 205, 179, and 200, respectively, and 20.2 ± 1.4 ka and > 47 ± 1.4 ka for leached samples of stones 205/200. Here, we studied two aliquots of stone 200 and measured ^{14}C specific activity concentrations of 0.66 ± 0.03 dpm kg^{-1} and 0.36 ± 0.02 dpm kg^{-1}. The weighted average value is 0.45 ± 0.14, that is, the 1σ standard deviation is ~31%. The bad reproducibility might be due to a small amount of contamination still remaining inside the crucible after the Qtz- and Pt crucibles needed to be replaced. Although the crucible was baked out multiple times and several system blanks were measured prior to Dho 005, we observed a slightly higher system and procedural blanks prior to the measurement of Dho005_001 (0.66 dpm kg^{-1}, lower ^{14}C age; also see Table S6). From the ^{14}C data, we calculate ^{14}C terrestrial ages of 35.8 ± 4.1 ka and 40.8 ± 4.5 ka, respectively (Table 3). The weighted average ^{14}C age is 38.1 ± 3.0 ka. The ^{14}C ages determined by us are similar to the published bulk age of the same Dho 005 sample and the ^{14}C activity concentrations determined by Al-Kathiri et al. (2005) are comparable to the ^{14}C

activity concentrations of the leached samples studied here.

There is one important aspect to remember. For long terrestrial ages, the effect of terrestrial ^{14}C production is no longer negligible, despite the fact that the production rate in space is orders of magnitude higher than on Earth. Assuming that the terrestrial production rate of ^{14}C is 1100 times lower than production in space (Jull et al., 2013; Lifton et al., 2001) we calculate from the saturation activity of ~50 dpm kg^{-1} for L-chondrites (see above), a terrestrial surface activity of ~0.05 dpm kg^{-1}. Consequently, from the 0.45 dpm kg^{-1} (weighted average of the two measurements), ~0.05 dpm kg^{-1} is from terrestrial production, leaving ~0.40 dpm kg^{-1} as the remaining ^{14}C activity for the meteorite. This change, however, would increase the ^{14}C terrestrial age only by ~1 ka.

Four ^{10}Be measurements of a homogenized ground sample of Dho 005 (stone 200) yielded ^{10}Be activity concentrations ranging from 14.4 to 14.8 dpm kg^{-1}, that is, the variability is 1%. The single ^{14}C-^{10}Be age, calculated from the mean ^{14}C (0.40 dpm kg^{-1}, corrected for terrestrial ^{14}C production; see above), is 35.4 ± 2.5 ka. Considering the good reproducibility of the ^{10}Be data, we consider this terrestrial age as the best estimate for this strewn field. Note that most of the weathering parameters also confirm that the terrestrial age of Dho 005 is larger than 30 ka (Al-Kathiri et al., 2005). Here, we confirm Dho 005's high terrestrial age and future measurements of other stones of the strewn field would help to distinguish whether variations in measured ^{14}C activity concentrations among the different samples are caused by differences in sample preparation (leaching process) or if they are due to real inhomogeneities in the strewn field.

Sayh al Uhaymir 163

Two replicate measurements of SaU 163 yielded ^{14}C specific activity concentrations of 2.80 ± 0.04 dpm kg^{-1} and 2.99 ± 0.05 dpm kg^{-1} (Table 3), that is, the variability is ~7%. The calculated ^{14}C terrestrial ages are 23.0 ± 3.1 ka and 22.5 ± 3.1 ka, respectively, with a mean value of 22.8 ± 2.2 ka. Al-Kathiri et al. (2005) measured a ^{14}C age of >50 ka for a leached aliquot of SaU 163. Interestingly, and as was also the case for Dho 005, the ^{14}C activity concentration of SaU 163 measured by Al-Kathiri et al. (2005) for the bulk sample is consistent with the ^{14}C activity concentration measured by us for the leached sample. In contrast, Al-Kathiri et al.'s data for leached aliquots are significantly different, that is (−0.47) ± 0.20 dpm kg^{-1} and 3.56 ± 0.15 dpm kg^{-1}.

The four ^{10}Be activity concentrations measured for a homogenized ground sample of SaU 163 range from 19.4 to 19.6 dpm kg^{-1}, that is, the variability is 0.2%. The ^{14}C-^{10}Be terrestrial age, calculated using the averages for ^{14}C and ^{10}Be, is 23.3 ± 2.0 ka, which is very close to the determined average ^{14}C age. We use this ^{14}C-^{10}Be age as the best estimate of the terrestrial age of SaU 163.

Ramlat as Sahmah 267

We measured two replicates from a homogenized ground sample of RaS 267 (see Table S8) and we determined ^{14}C activity concentrations of 2.25 and 2.22 dpm kg^{-1} (Table 3), that is, in a very good agreement. The thus calculated ^{14}C ages are almost identical at 26.3 ± 3.3 ka and 26.4 ± 3.4 ka. Zurfluh et al. (2016) measured a ^{14}C activity concentration of 1.4 dpm kg^{-1} for a leached aliquot of RaS 267, which gives a ^{14}C age of 30.5 ± 4.4 ka. The published age and the two ages measured by us agree within their uncertainties.

Four ^{10}Be measurements of a homogenized ground sample of RaS 267 yielded ^{10}Be activity concentrations in the range 14.3–14.5 dpm kg^{-1}. The average value is 14.4 ± 0.1 dpm kg^{-1}. The calculated ^{14}C-^{10}Be age of RaS 267 is 23.0 ± 2.0 ka in a very good agreement with the ^{14}C ages and is used for further discussion.

Ramlat as Sahmah 418

The RaS 418 strewn field has not been previously studied with respect to terrestrial ages. Here, we studied the two stones 153 and 32 for ^{14}C (Table S9) and ^{10}Be (Table S10); the other two stones 29 and 30 were only measured for ^{10}Be. For sample 153, we measured ^{14}C activity concentrations of 2.52 and 2.43 dpm kg^{-1}, that is, they agree within 4%. For the second sample 32, we measured 2.76 and 2.61 dpm kg^{-1}, that is, they also agree within 6%. From the measured activity concentrations, we calculate ^{14}C ages of 24.8 ± 3.3 ka and 25.1 ± 3.3 ka for sample 153, and 24.0 ± 3.2 ka and 24.5 ± 3.2 ka for sample 32. The average ^{14}C age is 24.6 ± 1.6 ka.

The ^{10}Be activity concentrations of the two stones of RaS 418 range from 19.0 to 19.5 dpm kg^{-1}. The ^{14}C-^{10}Be ages, calculated using an average of the ^{14}C activity concentrations and a single ^{10}Be activity concentration for each stone, are 24.5 ± 2.1 ka and 24.0 ± 2.1 ka for stones 153 and 32, respectively, that is, both ages are essentially identical. The mean ^{14}C-^{10}Be-age of RaS 418 of 24.2 ± 1.5 ka is taken as the best estimate of the terrestrial age for this strewn field.

^{14}C-^{10}Be Terrestrial Age Distribution

Based on previous work, the ^{14}C terrestrial age distribution of the ordinary chondrite population in Oman has a mean ^{14}C age of 21.0 ka (Zurfluh

et al., 2016) and is characterized by a prominent lack of young meteorites (<10 ka). This (unexpected) age distribution has been observed by Al-Kathiri et al. (2005) and Jull (2006). A similar (unexpected) ^{14}C age distribution has been observed for Roosevelt Country meteorites in the United States (Jull, 2006). In contrast, meteorite populations from other hot desert areas, such as western Australia and Algeria (Jull, 2006; Jull et al., 2010), show the expected (or approximately so) terrestrial age distribution, that is, an exponential decrease in the number of meteorites with increasing terrestrial age.

A histogram of the newly measured terrestrial ages of seven strewn fields of Omani ordinary chondrites studied by us is shown in Fig. 3, also including the two strewn fields Ghubara and Ramlat Fasad (RaF) 032 to provide as complete as possible picture of all the young strewn fields from Oman. With the current study, terrestrial ages for nine major strewn fields from Oman are available. Note that it is very likely that all major strewn fields in Oman have been discovered. It must be noted, however, that several smaller strewn fields have not yet been dated. The distribution previously determined by Zurfluh et al. (2016) has been normalized to the current sample size (n = 9) and is plotted in Fig. 3 for comparison. The average terrestrial age of the nine strewn fields is 15.9 ± 12.3 ka. The median is 13.6 ka. Based on the data from this study alone, this distribution also shows a lack of meteorites with terrestrial ages of <5 ka. One strewn field (SaU 001) falls in the 5–10 ka bin. In addition, the distribution shows a low abundance of strewn fields with terrestrial ages larger than 25 ka. Connected to this, while the previously published ^{14}C terrestrial age of SaU 163 was very high, >50 ka, the new ^{14}C and ^{14}C-^{10}Be terrestrial ages are significantly lower, that is, 22.8 ± 2.2 ka and 23.3 ± 2.0 ka, respectively. However, by including the Ghubara and RaF 032 strewn fields (both L ordinary chondrites) in the statistics, the lack of young strewn fields disappears and there might even be a slight peak at 0–15 ka. The Ghubara strewn field (total mass > 1750 kg, Meteoritical Society Database) has a young terrestrial age of 0.8–3.4 ka (Ferko et al., 2002; Jull et al., 2013), consistent with the low degree of weathering (W0-1; Al-Kathiri et al., 2005). The Ramlat Fasad 032 strewn field has an age of <1 ka (Rosén et al., 2021). Considering all nine dated strewn fields from Oman, the age distribution is closer to the one expected than based on previous work (Zurfluh et al., 2016).

By accepting the assumption of a constant meteorite flux and assuming constant, or at least almost constant, destruction of meteorites by erosion, we would expect an exponentially declining number of meteorites with increasing terrestrial age, that is, we would expect a high number of young meteorites/strewn fields and a decreasing number of meteorites/strewn fields with increasing terrestrial age. Figure 3 shows that by dating strewn fields, even at a much lower total number, the age distribution is closer to what we expect than by dating individual meteorites. However, old strewn fields may be underrepresented due to progressed erosion of meteorites, and the still low abundance of young individual meteorites discussed below remains unexplained.

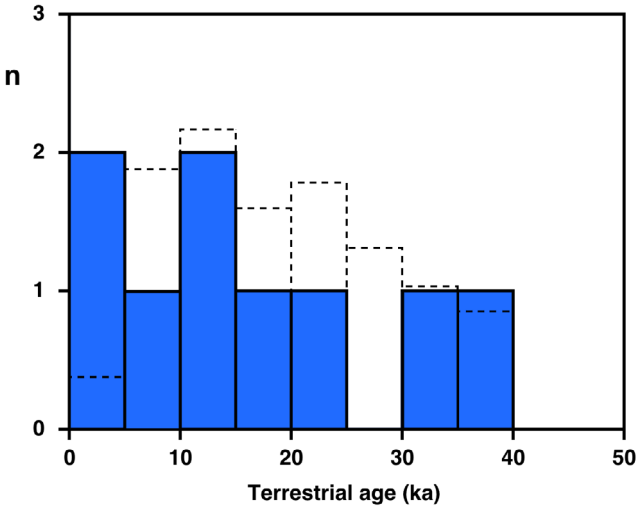

Fig. 3. Histogram of the best estimate (see text) terrestrial ages for the studied strewn fields and for the previously dated strewn fields Ghubara (Jull et al., 2013) and Ramlat Fasad 032 (Rosén et al., 2021). The dashed line indicates the terrestrial age distribution of individual meteorites (n = 128) previously determined by Zurfluh et al. (2016), normalized to the plotted sample size (n = 9). (Color figure can be viewed at wileyonlinelibrary.com.)

However, there might be an explanation for the apparent overabundance of moderately old meteorites in previous studies: There is not an overabundance of *moderately old* meteorites but an overabundance of ^{14}C in old meteorites. The source thereof would likely be terrestrial contamination that leaching/cleaning procedures are not able to remove entirely. There are two points relevant to this. First, for old and more weathered meteorites, the removal of terrestrial contamination becomes more difficult. Second, such old meteorites have low ^{14}C activity concentrations and are therefore relatively easy to compromise even by minor remaining contamination.

Comparison of ^{14}C and ^{14}C-^{10}Be Terrestrial Ages

Currently only a small database of ^{14}C-^{10}Be terrestrial ages for ordinary chondrites from Oman

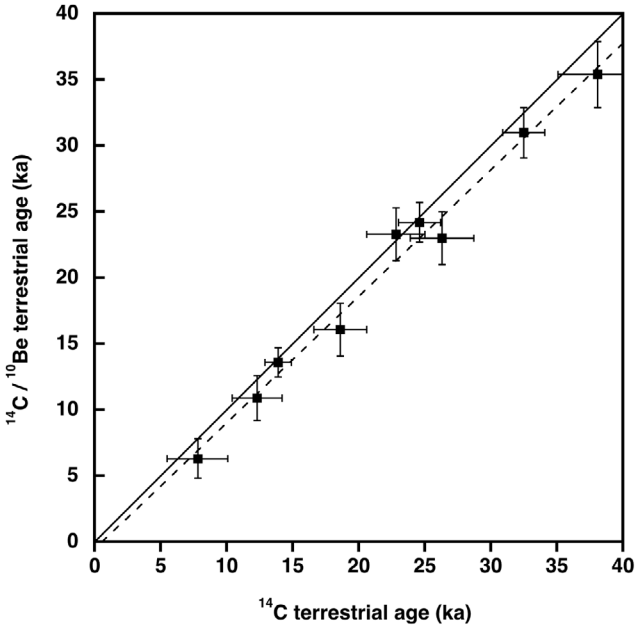

Fig. 4. ^{14}C-^{10}Be terrestrial ages as a function of ^{14}C terrestrial ages. There is a good linear correlation ($R = 0.992$) demonstrating the reliability of our study. The dotted line is the correlation fitted through the data, $T_{14/10} = -0.606 + 0.961\ T_{14}$.

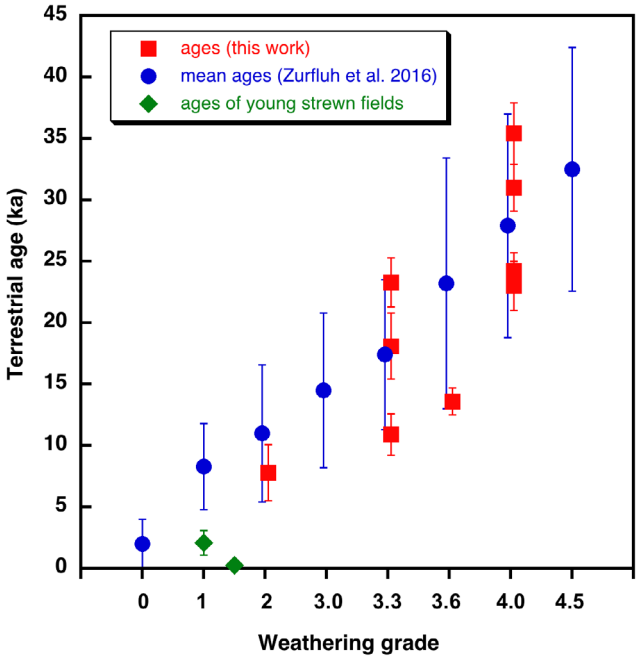

Fig. 5. Plot of the relation between the mean weathering grade (scale of Zurfluh et al., 2016) and our best-estimate terrestrial ages (squares). Circles are the mean ages for different weathering degrees from Zurfluh et al. (2016). Diamonds represent the young strewn fields Ramlat Fasad 032 (Rosén et al., 2021; see text) and Ghubara (Jull et al., 2013). Note that weathering grades are plotted as individual numerical classes.

exists. Before our study, ^{14}C-^{10}Be terrestrial ages were only available for samples from the JaH 073 strewn field, and unfortunately, those are less meaningful because of the complex exposure history of JaH 073. Considering that ^{14}C-^{10}Be terrestrial ages are more reliable than ^{14}C terrestrial ages (but sometimes less accurate, see also below) and that the interpretation of the terrestrial age histogram of strewn fields suffers from very low statistics, the database should definitely be extended.

Figure 4 depicts the mean ^{14}C-^{10}Be terrestrial ages as a function of the mean ^{14}C terrestrial ages for the samples studied by us (strewn field samples and individuals). First, there is a very good linear correlation between the two dating systems ($R = 0.992$). The precision is expected to be higher for the ^{14}C-^{10}Be ages because the ^{14}C/^{10}Be production rate ratio is much less dependent on shielding than the ^{14}C production rate, especially for large meteorites. Ages, and terrestrial and cosmic ray exposure are more reliable if they are corrected for shielding. For ^{10}Be-^{14}C ages to be reliable, ^{10}Be must be in saturation, which requires cosmic ray exposure ages larger than 7–8 Ma (Jull et al., 2013). If ^{10}Be is not in saturation at the time of fall, then the ^{14}C/^{10}Be ratio would be higher than the accepted value of ~2.5 (Jull et al., 2001; Kring et al., 2001; Welten et al., 2001) corresponding to a younger ^{14}C-^{10}Be age than the true terrestrial age of the sample. Therefore, ideally the determination of ^{14}C-^{10}Be terrestrial ages should be accompanied by a study of the cosmic ray exposure ages using, for example, cosmogenic noble gases.

Second, it can be seen that ^{14}C-^{10}Be ages are, on average, 7.8% lower than the ^{14}C ages. Since the slope of the correlation in Fig. 4 is close to 1, that is, there is a similar offset for all ages, the discrepancy is most likely in the ^{14}C production rates and/or ^{14}C/^{10}Be production rate ratio used for dating. Consequently, for reliable dating, there is a need to have better and more consistent knowledge on the ^{14}C and ^{10}Be production rates.

Correlation of Weathering Degree and Terrestrial Age

We use the best estimates for the terrestrial ages to compare them to the weathering degrees of the different samples/strewn fields (Fig. 5). For this study, that is, for correlating terrestrial ages to weathering degrees, strewn fields are particularly important. Sometimes different stones of the same strewn field have different weathering degrees and relating average or median

weathering degrees to terrestrial ages might be more representative than by using weathering degrees obtained from single stones. Figure 5 depicts the relationship between the degree of weathering and the best estimate of the terrestrial age. In addition, we also show the age-weathering relationship obtained by Zurfluh et al. (2016) on single samples. The plot also includes the strewn fields Ghubara (0.8–3.4 ka, Jull et al., 2013) and RaF 032 with a terrestrial age of 230 + 60/−30 yr based on measured ^{44}Ti activities; an age which is consistent with OSL-dating of underlying dune sand (Rosén et al., 2021).

Our new data show a good agreement, within uncertainties, with the relation between terrestrial age and weathering degree obtained by Zurfluh et al. (2016). Dhofar 020 (weathering grade 3.6) appears as an outlier. This may be due to the fact that for this meteorite, we collected only small stones (mean mass 16.5 g, n = 78). Likely, weathering proceeds faster in small stones than in larger ones, moving the data points too far to the right. Two findings are of importance. First, the ^{14}C data from this study and those in Zurfluh et al. (2016) were obtained in different laboratories, confirming the general reproducibility of the data. While the study by Zurfluh et al. (2016) has the advantage of being based on a larger number of individual samples, our new data can be considered more robust as both terrestrial age and weathering degree were obtained on multiple samples from strewn fields, all having the same terrestrial age. Second, the two data sets together demonstrate a well-established age-weathering correlation for south central Oman, with relatively large variations of terrestrial ages for individual weathering grades. Turning the argument around, there is a relatively large spread in weathering degree for the same terrestrial age. This clearly indicates that there are a number of influencing parameters such as porosity, size of meteorites, and local environmental differences affecting the weathering degree. Third, previously it has been recognized that there is a relatively low abundance of meteorites having a low degree of weathering in Oman (Al-Kathiri et al., 2005; Zurfluh et al., 2016). Since our study essentially confirms the relationship between weathering degree and terrestrial age, the lack of individual meteorites with low terrestrial age is confirmed by us, while strewn fields appear to be closer to the expected terrestrial age abundances. Since we can rule out analytical difficulties, we are left with the possibilities of (i) a change in meteorite flux over time or (ii) the common contamination of meteorites with terrestrial ^{14}C. Since a change in the meteorite flux over time appears unlikely, at least in the time frame studied here by us, we consider contamination as the most likely explanation. We will apply the systematic increase of weathering degree with age to obtain model age distributions for the complete collection of Oman meteorites. This requires a good knowledge of the pairing relationships of the recovered meteorites in order to base statistics on the number of recovered fall events. Due to differences in climatic conditions and climate histories of other hot desert environments, the degree of weathering increase with terrestrial age observed for Oman cannot be applied to other hot deserts.

CONCLUSIONS

Here, we present ^{14}C and ^{14}C-^{10}Be terrestrial ages of seven ordinary chondrite strewn fields and two unpaired single meteorites from Oman. Terrestrial ages obtained from the same stone of a strewn field show typically a good reproducibility. The reproducibility between different stones of the same strewn field is slightly worse but still good. In general, ^{14}C-^{10}Be ages are more accurate (but sometimes less precise) than ^{14}C ages. The following findings are important:

- Terrestrial ages are strongly correlated with weathering degree and the relation found by us is very similar to the one observed previously (Zurfluh et al., 2016).
- The previously observed lack of young meteorites, shown by Zurfluh et al. (2016) for individual meteorites, is indirectly supported by this study because of the similar relation between terrestrial ages and weathering degrees.
- By including the young strewn fields Ghubara and Ramlat Fasad 032, the histogram of strewn field ages shows a general slight decrease of abundance of ages up to 40 ka. The abundance of terrestrial ages of strewn fields alone appears to be closer to the expected exponential decrease with age, therefore, but also might include a sampling bias.
- While their number is much smaller, strewn fields represent large fall events and are therefore outstanding elements of the meteorite population providing multiple samples, particularly important for the relation between terrestrial age and weathering.
- Based on the ^{10}Be data, none of the investigated strewn fields appears to be derived from a meteoroid with a radius larger than ~150 cm, consistent with an estimated radius of 115 ± 15 cm for the largest investigated strewn field JaH 091 based on ^{26}Al (Weber et al., 2017).
- Determining terrestrial ages for a greater number of Omani meteorites would help to better constrain their terrestrial age histogram and thereby to better constrain the meteorite flux in the past. In the

absence of very large pre-atmospheric masses, ^{14}C ages alone would be suitable for this purpose.
- The relationship between terrestrial age and weathering, now firmly established, may be used in future studies to model the age distribution of all collected Oman meteorites under consideration of pairing.

Acknowledgments—This study was supported by Swiss National Science Foundation grant 200020_166251. We thank the Public Authority for Mining and the Ministry of Heritage and Tourism of the Sultanate of Oman for the support and necessary permissions during fieldwork. The ASTER AMS national facility (CEREGE, Aix-en-Provence) is supported by the INSU/CNRS, the ANR through the "Projets thématiques d'excellence" program for the "Equipements d'excellence" ASTER-CEREGE action, and IRD. Very constructive reviews by Kees Welten and Hamed Pourkhorsandi helped to significantly improve the manuscript.

Data Availability Statement—Data available on request from the authors.

Editorial Handling—Dr. A. J. Timothy Jull

REFERENCES

Aboulahris, M., Chennaoui Aoudjehane, H., Rochette, P., Gattacceca, J. R., Jull, A. J. T., Laridhi Ouazaa, N., Folco, L., and Buhl, S. 2019. Characteristics of the Sahara as a Meteorite Recovery Surface. *Meteoritics & Planetary Science* 54: 2908–28.

Al-Kathiri, A., Hofmann, B. A., Jull, A. J. T., and Gnos, E. 2005. Weathering of Meteorites from Oman: Correlation of Chemical and Mineralogical Weathering Proxies with Terrestrial Ages of the Influence of Soil Chemistry. *Meteoritics & Planetary Science* 40: 1215–39.

Arnold, M., Aumaitre, G., Bourlès, D. L., Keddadouche, K., Braucher, R., Finkel, R. C., Nottoli, E., Benedetti, L., and Merchel, S. 2013. The French Accelerator Mass Spectrometry Facility ASTER After 4 Years: Status and Recent Developments on ^{36}Cl and ^{129}I. *Nuclear Instruments and Methods in Physics Research Section B: Beam Interactions with Material and Atoms* 294: 24–9.

Arnold, M., Merchel, S., Bourlès, D. L., Braucher, R., Benedetti, L., Finkel, R. C., Aumaitre, G., Gottdang, A., and Klein, M. 2010. The French Accelerator Mass Spectrometry ASTER: Improved Performance and Developments. *Nuclear Instruments and Methods in Physics Research Section B: Beam Interactions with Material and Atoms* 268: 1954–9.

Bevan, A. W. R. 2006. Desert Meteorites: A History. In *The History of Meteoritics and the Key to Meteorite Collections: Fireballs, Falls and Finds. Geological Society London Special Publications* 256: 325–43. London: Geological Society of London.

Bevan, A. W. R., Bland, P. A., and Jull, A. J. T. 1998. Meteorite Flux on the Nullarbor Region, Australia. In *Meteorites: Flux with Time and Impact Effects*, edited by D. A. Rothery, vol. 140, 59–73. London: Geological Society of London.

Bischoff, A., and Geiger, T. 1995. Meteorites from the Sahara: Find Locations, Shock Classification, Degree of Weathering and Pairing. *Meteoritics* 30: 113–22.

Bland, P. A., Berry, F. J., Smith, T. B., Skinner, S. J., and Pillinger, C. T. 1996. The Flux of Meteorites to the Earth and Weathering in Hot Desert Ordinary Chondrite Finds. *Geochimica et Cosmochimica Acta* 60: 2053–9.

Born, W., and Begemann, F. 1975. ^{14}C-$^{39}Ar_{me}$ Correlations in Chondrites and their Pre-Atmospheric Size. *Earth and Planetary Science Letters* 25: 159–69.

Bourlès, D. L. 1988. Etude de la geochimie de l'isotope cosmogénique ^{10}Be et de son isotope stable ^{9}Be en milieu océanique. Application à la datation des sédiments marins. Ph.D. thesis, Paris-sud Centre d'Orsay, Paris, France.

Brown, E. T., Edmond, J. M., Raisbeck, G. M., Yiou, F., Kurz, M. D., and Brook, E. J. 1991. Examination of Surface Exposure Ages of Antarctic Moraines Using In Situ Produced ^{10}Be and ^{26}Al. *Geochimica et Cosmochimica Acta* 55: 2269–83.

Cassidy, W. A. 2003. *Meteorites, Ice, and Antarctica*. New York: Cambridge University Press.

Cornish, L., and Doyle, A. 1984. Use of Ethanolamine Thioglycolate in the Conservation of Pyritized Fossils. *Paleontology* 27: 421–4.

David, J.-C., and Leya, I. 2019. Spallation, Cosmic Rays, Meteorites, and Planetology. *Progress in Particle and Nuclear Physics* 109: 103711.

Drouard, A., Gattacceca, J., Hutzler, A., Rochette, P., Braucher, R., Bourlès, D., ASTER Team, et al. 2019. The Meteorite Flux of the Past 2 m.y. Recorded in the Atacama Desert. *Geology* 47: 673–6.

Edgell, H. S. 2006. *Arabian Deserts*. Dordrecht: Springer.

Ferko, T. E., Wang, M.-S., Hillegonds, D. J., Lipschutz, M. E., Hutchison, R., Franke, L., Scherer, P., et al. 2002. The Irradiation History of the Ghubara (L5) Regolith Breccia. *Meteoritics & Planetary Science* 37: 311–27.

Fookes, P. G., and Lee, E. M. 2009. Desert Environments of Inland Oman. *Geology Today* 25: 226–31.

Gattacceca, J., Valenzuela, M., Uehara, M., Jull, A. J. T., Giscard, M., Rochette, P., Braucher, R., et al. 2011. The Densest Meteorite Collection Area in Hot Deserts: The San Juan Meteorite Field (Atacama Desert, Chile). *Meteoritics & Planetary Science* 46: 1276–87.

Gnos, E., Eggimann, M., Al-Kathiri, A., and Hofmann, B. A. 2006. The JaH 091 Strewnfield. *Meteoritics & Planetary Science* 41: A64–230.

Gnos, E., Lorenzetti, S., Eugster, O., Jull, A. J. T., Hofmann, B. A., Al-Kathiri, A., and Eggimann, M. 2009. The Jiddat al Harasis 073 Strewn Field, Sultanate of Oman. *Meteoritics & Planetary Science* 44: 375–87.

Grossman, J. N. 2000. The Meteoritical Bulletin, No. 84. *Meteoritics & Planetary Science* 35: A199–225.

Halliday, I., Blackwell, A. T., and Griffin, A. A. 1989. The Flux of Meteorites on the Earth's Surface. *Meteoritics* 24: 173–8.

Hezel, D. C., Schlüter, J., Kallweit, H., Jull, A. J. T., Fakeer, O. Y. A., Shamsi, M. A., and Strekopytov, S. 2011. Meteorites from the United Arab Emirates: Description, Weathering, and Terrestrial Ages. *Meteoritics & Planetary Science* 46: 327–36.

Hippe, K., Kober, F., Wacker, L., Fahrni, S. M., Ivy-Ochs, S., Akar, N., Schlüchter, C., and Wieler, R. 2013. An Update on In Situ Cosmogenic ^{14}C Analysis at ETH Zürich. *Nuclear Instruments and Methods in Physics Research B* 294: 81–6.

Hippe, K., and Lifton, L. 2014. Calculating Isotope Ratios and Nuclide Concentrations for In Situ Cosmogenic ^{14}C Analyses. *Radiocarbon* 56: 1167–74.

Hofmann, B. A. 2010. Meteorites: Messengers from the Early Solar System. *Chimia* 64: 736–40.

Hofmann, B. A., Gnos, E., and Al-Kathiri, A. 2003. Harvesting Meteorites in the Omani Desert: Implications for Astrobiology. Proceedings, III European Workshop on Exo-Astrobiology, Madrid, 10–20 November 2003 (ESA SP-545), 73–6.

Hofmann, B. A., Gnos, E., Eggenberger, U., Zurfluh, F. J., Boschetti, S., and Al-Rahji, A. 2011. The Omani-Swiss Meteorite Search Project—Recent Campaigns and Outlook. *Meteoritics & Planetary Science* 46: A97.

Hofmann, B. A., Gnos, E., Greber, N. D., Federspiel, N., Burri, T., Zurfluh, F. J., Al-Battashi, M., and Al-Rajhi, A. 2014. The Omani-Swiss Meteorite Search Project: Update and the Quest for Missing Irons. *Meteoritics & Planetary Science* 49: A170.

Hofmann, B. A., Gnos, E., Jull, A. J. T., Szidat, S., Majoub, A., Al Wagdani, K., Habibullah Siddiq, N., et al. 2018. Meteorite Reconnaissance in Saudi Arabia. *Meteoritics & Planetary Science* 53: 2372–94.

Huber, L., Gnos, E., Hofmann, B., Welten, K. C., Nishiizumi, K., Caffee, M. W., Hillegonds, D. J., and Leya, I. 2008. The Complex Exposure History of the Jiddat al Harasis 073 L-Chondrite Shower. *Meteoritics & Planetary Science* 43: 1691–708.

Hutzler, A., Gattacceca, J., Rochette, P., Braucher, R., Carro, B., Christensen, E. J., Cournede, C., et al. 2016. Description of a Very Dense Meteorite Collection Area in Western Atacama: Insight into the Long-Term Composition of the Meteorite Flux to Earth. *Meteoritics & Planetary Science* 51: 468–82.

Jull, A. J. T. 2006. Terrestrial Ages of Meteorites. In *Meteorites and the Early Solar System II*, edited by D. Lauretta, and H. Y. McSween, Jr., 889–905. Tucson, Arizona: The University of Arizona Press.

Jull, A. J. T., Bland, P. A., Bevan, A. W. R., Klandrud, S. E., and McHargue, L. R. 2001. ^{14}C and ^{14}C-^{10}Be Terrestrial Ages of Meteorites from Western Australia. *Meteoritics & Planetary Science* 36: A91.

Jull A. J. T., Cielaszyk E., and Cloudt, S. 1998. ^{14}C Terrestrial Ages of Meteorites from Victoria Land, Antarctica and the Infall Rates of Meteorites. In *Meteorites: Flux with Time and Impact Effects. Geological Society of London Special Publication* 140: 75–91. London: Geological Society of London.

Jull, A. J. T., Courtney, C., Jeffrey, D. A., and Beck, J. W. 1998. Isotopic Evidence for a Terrestrial Source of Organic Compounds Found in Martian Meteorites Allan Hills 84001 and Elephant Moraine 79001. *Science* 279: 366–9.

Jull, A. J. T., Donahue, D. J., Cielaszyk, E., and Wlotzka, F. 1993. Carbon-14 Terrestrial Ages and Weathering of 27 Meteorites from the Southern High Plains and Adjacent Areas (USA). *Meteoritics & Planetary Science* 28: 188–95.

Jull, A. J. T., Donahue, D. J., and Linick, T. W. 1989. Carbon-14 Activities in Recently Fallen Meteorites and Antarctic Meteorites. *Geochimca et Cosmochimica Acta* 53: 1295–300.

Jull, A. J. T., Giscard, M. D., Hutzler, A., Schnitzer, C. J., Zahn, D., Burr, G. S., McHargue, L. R., and Hill, D. 2013. Radionuclide Studies of Stony Meteorites from Hot Deserts. *Radiocarbon* 55: 1779–89.

Jull, A. J. T., McHargue, L. R., Bland, P. A., Greenwood, R. C., Bevan, A. W., Kim, K. J., LaMotta, S. E., and Johnson, J. A. 2010. Terrestrial Ages of Meteorites from the Nullarbor Region, Australia, Based on ^{14}C and ^{14}C-^{10}Be Measurements. *Meteoritics & Planetary Science* 45: 1271–83.

Jull, A. J. T., Wlotzka, F., Palme, H., and Donahue, D. J. 1990. Distribution of Terrestrial Age and Petrologic Type of Meteorites from Western Libya. *Geochemica et Cosmochemica Acta* 54: 2895–8.

Korochantsev, A. V., Sadilenko, D. A., Ivanova, M. A., Lorentz, C. A., and Zabalueva, E. V. 2003. A Study of the Fragment Dispersal and Trajectory of the Sayh al Uhaymir 001 Meteorite Shower. *Meteoritics & Planetary Science* 38: 5049.

Korschinek, G., Bergmaier, A., Faestermann, T., Gerstmann, U. C., Knie, K., Rugel, G., Wallner, A., et al. 2010. A New Value for the Half-Life of ^{10}Be by Heavy-Ion Elastic Recoil Detection and Liquid Scintillation Counting. *Nuclear Instruments and Methods in Physics Research B* 268: 187–91.

Kring, D. A., Jull, A. J. T., McHargue, L. R., Bland, P. A., Dolores, H. H., and Berry, F. J. 2001. Gold Basin Meteorite Strewn Field, Mojave Desert, Northwestern Arizona: Relic of a Small Late Pleistocene Impact Event. *Meteoritics & Planetary Science* 36: 1057–66.

Laridhi Ouazaa, N., Perchiazzi, N., Kassaa, S., Zeoli, A., Ghanmi, M., and Folco, L. 2009. Meteorite Finds from Southern Tunisia. *Meteoritics & Planetary Science* 44: 955–60.

Le Métour, J., Platel, J.-P., Béchennec, F., Berthiaux, A., Chevrel, S., Dubreuilh, J., Roger, J., and Wyns, R. 1993. Geological Map of the Sultanate of Oman. Scale 1:1.000.000. Directorate General of Minerals, Ministry of Petroleum and Minerals, Muscat.

Lee, N. N., Fritz, J., Fries, M. D., Gil, J. F., Beck, A., Pellinen-Wannberg, A., Schmitz, B., Steele, A., and Hofmann, B. A. 2017. The Extreme Biology of Meteorites: Their Role in Understanding the Origin and Distribution of Life on Earth and in the Universe. In *Adaption of Microbial Life to Environmental Extremes*, edited by H. Stan-Lotter and S. Fendrihan, 2nd ed., 283–325. Cham, Switzerland: Springer.

Leya, I., Ammon, K., Cosarinsky, M., Dalcher, N., Gnos, E., Hofmann, B. A., and Huber, L. 2013. Light Noble Gases in 12 Meteorites from Omani Desert, Australia, Mauritania, Canada, and Sweden. *Meteoritics & Planetary Science* 48: 1401–14.

Leya, I., and Masarik, J. 2009. Cosmogenic nuclides in stony meteorites revisited. *Meteoritics and Planetary Science* 44: 1061–86.

Leya, I., Neumann, S., Wieler, R., and Michel, R. 2001. The Production of Cosmogenic Nuclides by Galactic Cosmic-Ray Particles for 2π Exposure Geometries. *Meteoritics & Planetary Science* 36: 1547–61.

Lifton, N. A., Jull, A. J. T., and Quade, J. 2001. A New Extraction Technique and Production Rate Estimate for In Situ Cosmogenic ^{14}C in Quartz. *Geochimica et Cosmochimica Acta* 65: 1953–69.

Makjanic, J., Vis, R. D., Hovenier, J. W., and Heymann, D. 1993. Carbon in the Matrices of Ordinary Chondrites. *Meteoritics & Planetary Science* 28: 63–70.

Matter, A., Neubert, E., Preusser, F., Rosenberg, T., and Al-Wagdani, K. 2015. Palaeoenvironmental Implications Derived from Lake and Sabkha Deposits of the Southern Rub'al-Khali, Saudi Arabia and Oman. *Quaternary International* 382: 120–31.

Mészáros, M., Leya, I., Hofmann, B. A., and Szidat, S. 2018. Current Performance and Preliminary Results of a New ^{14}C Extraction Line for Meteorites at the University of Bern. *Radiocarbon* 60: 601–15.

Minami, M., and Nakamura, T. 2001. An Extraction System to Measure Carbon-14 Terrestrial Ages of Meteorites with a Tandetron AMS at Nagoya University. *Radiocarbon* 43: 263–9.

Minami, M., Terui, A., Takaoka, N., and Nakamura, T. 2006. An Improved Extraction System to Measure Carbon-14 Terrestrial Ages of Meteorites and Pairing of the Antarctic Yamato 75097 Group Chondrites. *Meteoritics & Planetary Science* 41: 529–40.

Munayco, P., Munayco, J., Avillez, R. C., Valenzuela, M., Rochette, P., Gattacceca, J., and Scorzelli, R. B. 2013. Weathering of Ordinary Chondrites from the Atacama Desert, Chile, by Mössbauer Spectroscopy and Synchrotron Radiation X-Ray Diffraction. *Meteoritics & Planetary Science* 48: 457–73.

Muñoz, C., Guerra, N., Martinez-Frias, J., Lunar, R., and Cerda, J. 2007. The Atacama Desert: A Preferential Arid Region for the Recovery of Meteorites—Find Location Features and Strewnfield Distribution Patterns. *Journal of Arid Environments* 71: 188–200.

Nishiizumi, K. 1995. Terrestrial Ages of Meteorites from Cold and Hot Deserts. Proceedings, Workshop on Meteorites from Cold and Hot Deserts. 53–5.

Nishiizumi, K., Elmore, D., and Kubik, P. W. 1989. Update on Terrestrial Ages of Antarctic Meteorites. *Earth and Planetary Science Letters* 93: 299–313.

Nishiizumi, K., Imamura, M., Caffee, M. W., Southon, J. R., Finkel, R. C., and McAninch, J. 2007. Absolute Calibration of ^{10}Be AMS Standards. *Nuclear Instruments and Methods in Physics Research Section B: Beam Interactions with Materials and Atoms* 258: 403–13.

Pourkhorsandi, H., Gattacceca, J., Rochette, P., D'Orazio, M., Kamali, H., de, Avillez, R., Letichevsky, S., et al. 2019. Meteorites from the Lut Desert (Iran). *Meteoritics & Planetary Science* 54: 1737–63.

Reedy, R. C., and Arnold, J. R. 1972. Interaction of Solar and Galactic Cosmic-Ray Particles with the Moon. *Journal of Geophysical Research* 77: 537–55.

Rosén, Å. V., Hofmann, B. A., Preusser, F., Gnos, E., Eggenberger, U., Schumann, M., and Szidat, S. 2021. Meteorite Terrestrial Ages in Oman Based on Gamma Spectrometry and Sediment Dating, Focusing on the Ramlat Fasad Dense Collection Area. *Meteoritics & Planetary Science* 56: 2017–34.

Schlüter, J., Schultz, L., Thiedig, F., Al-Mahdi, B. O., and Abu Aghreb, A. E. 2002. The Dar al Gani Meteorite Field (Libyan Sahara): Geological Setting, Pairing of Meteorites, and Recovery Density. *Meteoritics & Planetary Science* 37: 1079–93.

Sliz, M. U., Braucher, R., Espic, C., Gattacceca, J., Hofmann, B. A., Leya, I., Szidat, S., and ASTER Team. 2019. Terrestrial Ages of the Shişr 015 Meteorite Strewn Field from the Sultanate of Oman, Determined Using Measured In Situ ^{14}C and ^{10}Be. *Meteoritics & Planetary Science* 54 (S2): 6287.

Sliz, M. U., Braucher, R., Gattacceca, J., Hofmann, B. A., Jull, A. J. T., Leya, I., Szidat, S., and ASTER Team. 2018. Terrestrial Ages of Meteorites Using In Situ ^{14}C and ^{10}Be Measurements. *Meteoritics & Planetary Science* 53 (S1): 6297.

Sliz, M. U., Espic, C., Hofmann, B. A., Leya, I., and Szidat, S. 2020. An Update of the Performance of the In Situ ^{14}C Extraction Line at the University of Bern. *Radiocarbon* 62: 1371–88. https://doi.org/10.1017/RDC.2020.38.

Szidat, S., Salazar, G. A., Vogel, E., Battaglia, M., Wacker, L., Synal, H. A., and Türler, A. 2014. ^{14}C Analysis and Sample Preparation at the New Bern Laboratory for the Analysis of Radiocarbon with AMS (LARA). *Radiocarbon* 56: 561–6.

Weber, P., Hofmann, B. A., Tolba, T., and Vuilleumier, J.-L. 2017. A Gamma-Ray Spectroscopy Survey of Omani Meteorites. *Meteoritics & Planetary Science* 52: 1017–29.

Welten, K. C., Nishiizumi, K., Masarik, J., Caffee, M. W., Jull, A. J. T., Klandrud, S. E., and Wieler, R. 2001. Neutron-Capture Production of Chlorine-36 and Calcium-41 in Two H-Chondrite Showers from Frontier Mountain, Antarctica. *Meteoritics & Planetary Science* 36: 301–17.

Wlotzka, F. 1993. A Weathering Scale for the Ordinary Chondrites. *Meteoritics & Planetary Science* 28: 460–153.

Zolensky, M. E., Wells, G. E., and Rendell, H. M. 1990. The Accumulation Rate of Meteorite Falls at the Earth's Surface: The View from Roosevelt County, New Mexico. *Meteoritics* 25: 11–7.

Zurfluh, F., Hofmann, B., Gnos, E., Eggenberger, U., and Preusser, F. 2011. When Did the Large Meteorite Shower Jiddat al Harasis 091 Arrive on Earth? 9th Swiss Geoscience Meeting, Zurich, Switzerland.

Zurfluh, F. J., Hofmann, B. A., Gnos, E., Eggenberger, U., and Jull, A. J. T. 2016. Weathering of Ordinary Chondrites from Oman: Correlation of Weathering Parameters with ^{14}C Terrestrial Ages and a Refined Weathering Scale. *Meteoritics & Planetary Science* 51: 1685–700.

SUPPORTING INFORMATION

Additional supporting information may be found in the online version of this article.

Fig. S1. a–g) Individual stones of the studied strewn fields are plotted, showing their distribution as collected in the field. Sizes of symbols are scaled according to the mass of the stones. Terrestrial age dated samples are labeled and color coded: black—meteorites studied in this work only; red—meteorites studied by other authors only; and green—meteorites studied in this work and with terrestrial age data available in the literature.

Table S1. Complete ^{14}C data for the system blanks, procedural blanks, and samples of the JaH 073 strewn field.

Table S2. Complete ^{14}C data for the system blanks, procedural blanks, and samples of the Shişr 015 strewn field.

Table S3. Complete ^{14}C data for the system blanks, procedural blanks, and samples of the JaH 091 strewn field.

Table S4. Complete ^{14}C data for the system blanks, procedural blanks, and samples of the Dho 020 strewn field.

Table S5. Complete ^{14}C data for the system blanks, procedural blanks, and samples of the SaU 001 strewn field.

Table S6. Complete ^{14}C data for the system blanks, procedural blanks, and samples of the Dho 005 strewn field.

Table S7. Complete ^{14}C data for the system blanks, procedural blanks, and samples of the SaU 163 strewn field.

Table S8. Complete ^{14}C data for the system blanks, procedural blanks, and samples of the RaS 267 strewn field.

Table S9. Complete ^{14}C data for the system blanks, procedural blanks, and samples of the RaS 418 strewn field.

Table S10. ^{10}Be data for the measured strewn fields and two single meteorites presented in the same chronological order as ^{14}C and $^{14}C/^{10}Be$ terrestrial age data.